Table 1. *In vitro* growth inhibitory activity of SN-38, NK012, and CPT-11 in RCC lines (MTT assay)

Cell line	IC_{50} (μmol/L)		
	SN-38	NK012*	CPT-11
SKRC-49	0.0064 ± 0.005	0.011 ± 0.008	4.14 ± 0.45
Caki-1	0.0062 ± 0.009	0.032 ± 0.006	8.45 ± 0.85
769P	0.015 ± 0.007	0.085 ± 0.014	34.54 ± 3.76
786O	0.031 ± 0.007	0.12 ± 0.012	28.14 ± 1.21
KU19-20	0.10 ± 0.006	0.34 ± 0.014	32.65 ± 1.25
Renca	0045 ± 0.005	0.0096 ± 0.008	2.26 ± 0.05

*The dose of NK012 is expressed as a dose equivalent to SN-38.

Ltd. Monoclonal anti-CD34 antibody (HyCult Biotechnology) was used to detect the tumor blood vessels. CD34-positive neovessels were counted in 10 high-power fields (×400) by two independent investigators who operated in a blinded fashion.

Assay for free (polymer-unbound) SN-38 in lung tissues. The Renca pulmonary metastasis model described above was used for the analysis of the biodistribution of NK012 and CPT-11. Ten days after Renca inoculation, NK012 (20 mg/kg) or CPT-11 (30 mg/kg) was given i.v. to the mice. The mice were sacrificed at 0, 24, 48, and 72 h after administration, and lung samples were taken and stored at −80°C until analysis. We prepared control mice without Renca inoculation as the nonmetastatic model; NK012 was administrated as well, and lung samples were stored. Samples were then homogenized on ice using a Digital homogenizer (Iuchi) and suspended in the mixture of 100 mmol/L glycine-HCl buffer (pH 3)/methanol (1:1, v/v) at a concentration of 5% w/w. Proteins were precipitated with an ice-cold mixture of 1 mmol/L H_3PO_4/MeOH/H_2O (1:1:4, v/v/v) containing camptothecin as an I.S. The sample was vortexed for 10 s and filtered through a MultiScreen Solvinert (Millipore Corporation), and the concentration of free SN-38 in the aliquots of the homogenates (100 μL) was determined using the high-performance liquid chromatography method (6).

Statistical analysis. Data were expressed as mean ± SD. Significance of differences was calculated using the unpaired *t* test with repeated measures of StatView 5.0. $P < 0.05$ was regarded as statistically significant.

Results and Discussion

We first evaluated *in vitro* cellular sensitivity of RCC lines to SN-38, NK012, and CPT-11. The IC_{50} values of each agent for RCC lines are shown in Table 1. NK012 exhibited higher cytotoxic effect against each cell line compared with CPT-11 (96-fold to 406-fold sensitive).

It is essential to elucidate the correlation between the effectiveness of micellar drugs and tumor hypervascularity and hyperpermeability. Gross evaluation of those RCC tumors s.c. injected into the backs of mice revealed that Renca tumors were more reddish and grew faster than SKRC-49 tumors, and immunohistochemical examination showed that Renca tumors contained much more CD34-positive neovessels than SKRC-49 tumors (Fig. 1).

We allowed the tumors to grow until they became massive, around 1.5 cm, and then initiated treatment. A striking decrease in Renca tumor volume was observed on day 15 in mice treated with NK012 at 20 mg/kg/d compared with the untreated control (Fig. 2*A*). Renca bulky masses completely disappeared on day 21 in 6 of 10 mice treated with NK012 at 20 mg/kg/d. On the other hand, Renca tumors in mice treated with CPT-11 at 30 mg/kg/d were not eradicated and rapidly regrew after a partial response at day 15. An approximate 10% body weight loss occurred in mice treated with NK012 20 mg/kg, compared with the untreated controls, but there was no significant difference in comparison with tumor-free mice treated with NK012, suggesting that the decrease in body weight was likely to be due to tumor shrinkage rather than toxic effects. We next compared the antitumor activities of the NK012 and CPT-11 treatment in SKRC-49 and Renca tumors. The SKRC-49 tumor volume in mice treated with NK012 at 20 mg/kg/d on day 21 was over 70% smaller than in the untreated controls on day 21 and ~50% smaller than in mice on day 0 (Fig. 2*B*). However, the SKRC-49 tumors were not eradicated in mice treated with NK012. Considering that equivalent *in vitro* growth inhibitory effects by NK012 were observed for SKRC-49 and Renca cells (Table 1), our results suggest that the antitumor activity of NK012 *in vivo* might be affected by tumor environment factors, such as tumor vascularity.

We next examined the distribution of free SN-38 in the metastatic or nonmetastatic (no inoculation of Renca cells) lung tissues after administration of NK012 or CPT-11. In the case of NK012 administration in mice with lung metastasis, free SN-38 was detectable at the concentration of >100 ng/g in metastatic lung tissues with a typical microvascular architecture (Fig. 3*A*) even at 72 hours after administration, whereas the concentrations of free SN-38 in nonmetastatic lung tissues after NK012 administration were much lower than those in metastatic lung tissues after treatment with NK012 (significant at 24, 48, and 72 hours; $P < 0.05$;

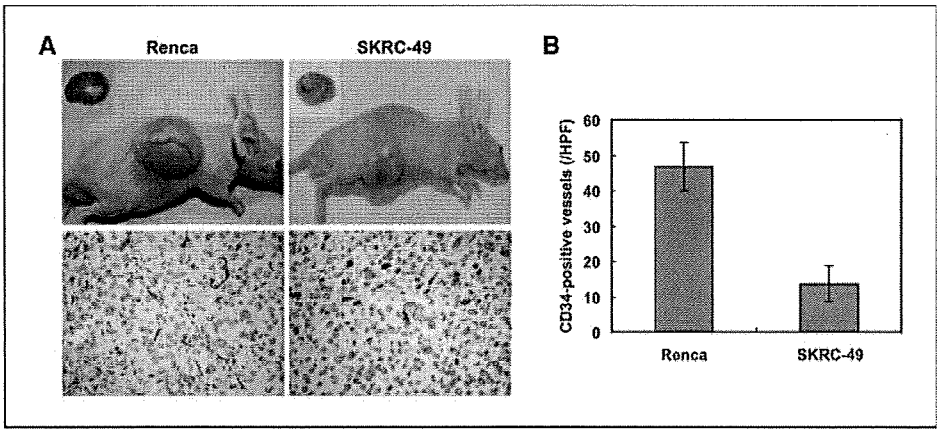

Figure 1. Comparison of tumor angiogeneses of Renca and SKRC-49 in athymic nude mice. *A*, representative photographs of massive tumors developed from Renca and SKRC-49 at 28 d after s.c. injection (inoculation). Immunohistochemical (CD34, ×400) examinations for each tumor are shown. *B*, tumor neovascularization in each tumor was quantified by counting CD34-positive neovessels. *Bars*, SD. Experiments were repeated twice with similar results.

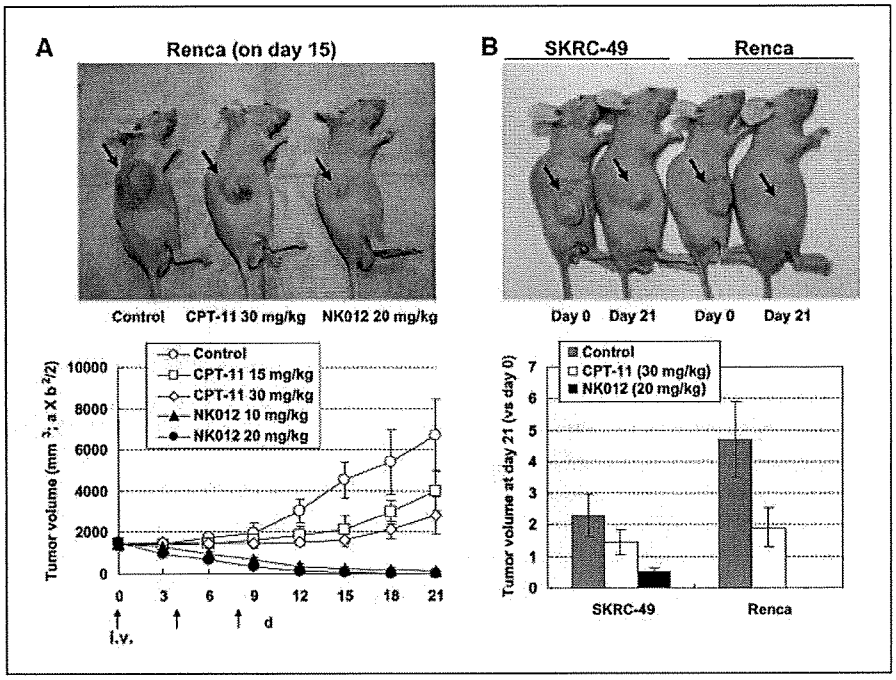

Figure 2. Growth-inhibitory effect of NK012 and CPT-11 on bulky RCC tumors. I.v. administration of NK012 or CPT-11 was started when the mean tumor volumes of groups reached a massive 1,500 mm^3. The mice were divided into test groups as indicated. *A*, representative of each group at day 15 in the Renca allograft model. *Arrows*, Renca allografts (*top*). Time profile of tumor volume in mice treated with NK012 or CPT-11 at indicated doses (*bottom*). Each group consisted of 10 mice. *Bars*, SD. *B*, the comparison of antitumor activities of CPT-11 and NK012 in SKRC-49 xenografts and Renca allografts. Representative of mice treated with NK012 at day 0 and day 21. Experiments were repeated twice with similar results. The mice at day 0 in the photograph belong to the group in the second experiment which started just at day 21 of the first experiment. *Arrows*, tumor grafts. The relative tumor volume values at day 21 to those at day 0 in each group set to 1 (*bottom*). Each group consisted of 10 mice.

Fig. 3*B*). On the other hand, the concentrations of free SN-38 after administration of CPT-11 were almost negligible in metastatic lung tissues at all time points (data not shown). These results strongly suggest that SN-38 could be selectively released from NK012 and maintained in metastatic Renca tumor tissues.

Deviating from the ordinary experimental pulmonary metastasis prevention model, we initiated treatment 7 days after inoculation (day 0) when multiple lung nodules derived from Renca were observed in all mice in our preliminary study (Fig. 4*A*). On day 21, there was no significant difference between the mean number of metastatic nodules in the control group (287 ± 56 nodules, $n = 10$) and in the group receiving CPT-11 treatment (236 ± 59 nodules, $n = 10$). Significant treatment effects were found, however, in the group receiving NK012 treatment (32 ± 18 nodules, $n = 10$) on day 21 compared with the control group on day 21 ($P < 0.0001$). Notably, a dramatic decrease in metastatic nodule number was observed in the NK012 treatment group on day 21 compared with the control group on day 0 (126 ± 23 nodules, $n = 10$, $P < 0.001$; Fig. 4*A*). Kaplan-Meier analysis showed that a significant survival benefit was obtained in the NK012 treatment group compared with

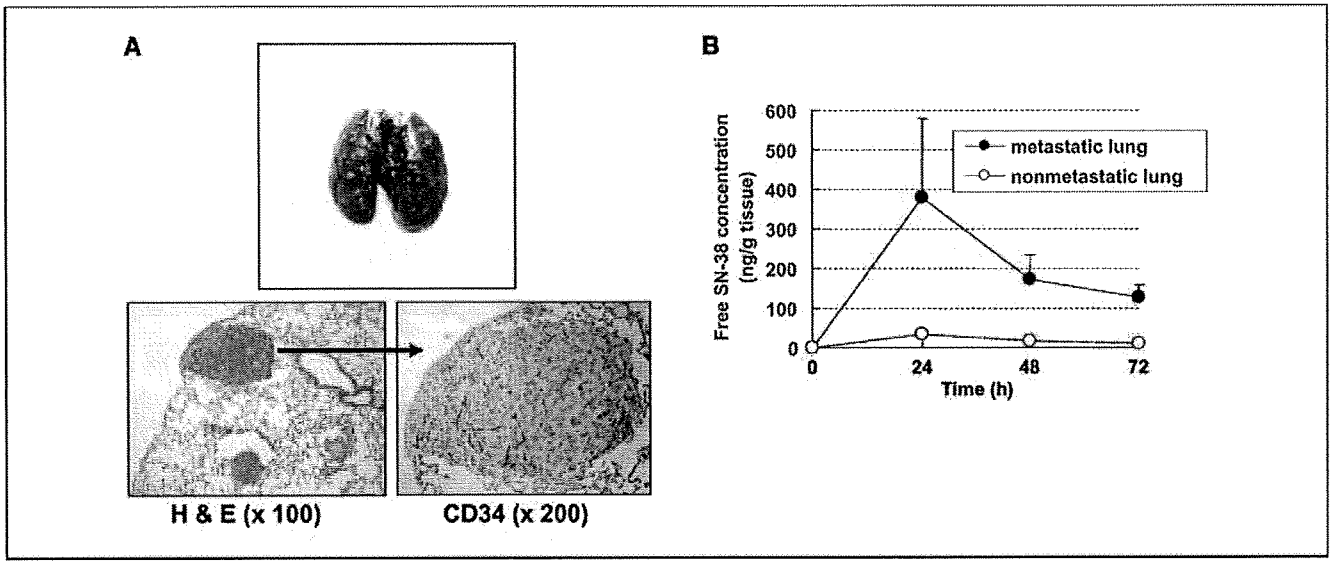

Figure 3. Pulmonary metastasis of Renca cells and lung tissue distribution of free SN-38 after administration of NK012 and CPT-11. *A*, gross appearances of pulmonary metastasis observed 7 d after Renca inoculation (*top*). Multiple metastatic nodules and neovascularization in metastatic lung tumor lesion (*bottom*). *B*, time profile of free SN-38 concentration in metastatic or nonmetastatic lung tissues in mice treated with NK012 (20 mg/kg/d). *Bars*, SD. Experiments were performed in tetraplicate.

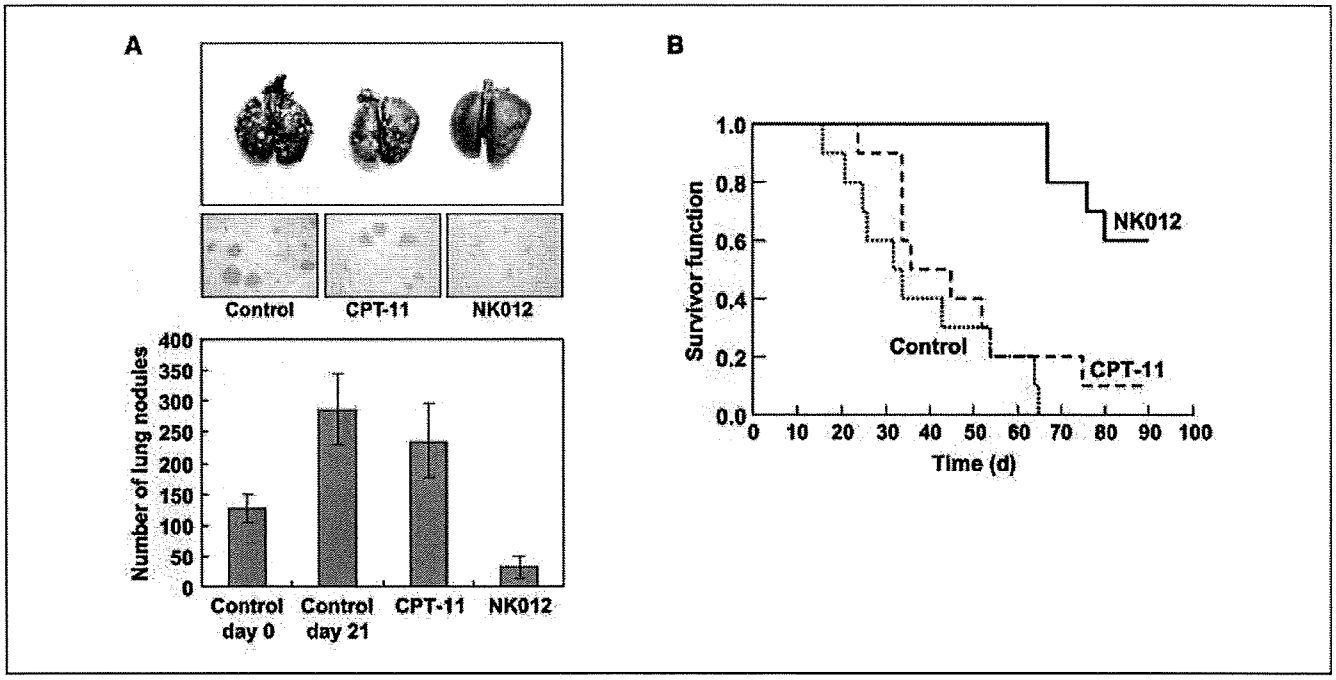

Figure 4. Treatment effect of NK012 on established pulmonary metastasis and survival. NK012 (20 mg/kg/d) and CPT-11 (30 mg/kg/d) were given i.v. to mice with established pulmonary metastasis on days 0 (7 d after Renca inoculation), 4, and 8. *A*, gross and histologic appearances of pulmonary metastases at day 21 (*top*). The metastatic nodules in each mouse were counted. Each group consisted of five mice. *B*, mice were maintained for 90 d after each treatment and survival was assessed by a Kaplan-Meier analysis. Each group consisted of five mice. Experiments were repeated twice with similar results.

the control group ($P < 0.001$), but no significant survival benefit was obtained in CPT-11 treatment group ($P = 0.239$; Fig. 4*B*). Although no severe toxic effects were observed in any mouse treated with NK012, 3 of 10 mice treated with NK012 were sacrificed during the observation period according to the 'Guidelines for Animal Experiments because their body weights had become 10% lower than those of the other mice. However, the sacrificed mice were a little bit smaller than others when they started treatment, and they showed no disseminated lung metastasis (data not shown).

Our results presented here strongly support recent findings reported by us that the macromolecular drug distribution throughout the tumor site was enhanced by the hypervascularity and hyperpermeability, and subsequently higher antitumor activity was achieved (6). We assume that conventional low molecular size anticancer agents almost disappear from the bloodstream without being subjected to the EPR effect before they can reach the target organs (solid tumor). The clinical importance of angiogenesis in human tumors has been shown in several reports indicating a positive relationship between the blood vessel density in the tumor mass and poor prognosis with chemoresistance in patients with various cancers (7–9). Furthermore, recent reports showing that anticancer agents were less active against VEGF-overexpressing tumors (10, 11) may support the idea that low-molecular drugs are not so effective in the treatment of solid tumors which are rich in blood vessels.

Our study thus far has several limitations about clarifying whether extensive angiogenesis in the tumor is an essential determinant for the susceptibility to NK012. In our ongoing study, we found that NK012 also has a striking antitumor activity against some hypovascular tumor models of human pancreatic cancer xenografts.[5] It also remains unclear whether NK012 possesses strong antitumor activity in other metastatic sites besides the lung. It is known that the EPR effect is affected by various permeability factors, such as bradykinin (12), nitric oxide (13). and various cytokines independent of VEGF and hypervascularity (14). Among solid tumors with rapid progression potential, irregularity occurs not only in blood flow and vascular density, but also in the vascular network and anatomic architecture (15, 16), suggesting that EPR effect may be predominantly promoted in rapid-progressive tumor phenotypes and influenced by organ-specific tumor microenvironment. Hoffman and coworkers (17, 18) have developed a technique of surgical orthotopic implantation (SOI) with more clinical features of systemic and aggressive metastases than our conventional animal models. Further preclinical studies using such models as SOI might clarify cancer phenotypes and metastatic organs to which we can apply NK012 more precisely.

The results of chemotherapy in RCCs have been disappointing, as indicated by the low response proportions. However, clinical trials using gemcitabine-containing regimens have been encouraging, with major responses occurring in 5% to 17% of patients (19, 20), suggesting the possibility that chemotherapy is promising as a modality for RCC therapy if anticancer agents can be selectively delivered, released, and maintained around tumor tissues. Our current report highlights the advantages of polymeric micelle-based drug carriers like NK012 as promising modalities for treatment, rather than prevention, of disseminated RCCs with abnormal vascular architecture. The results of our ongoing phase-I

[5] Y. Saito, M. Yasumaga, J. Kuroda, Y. Koga, and Y. Matsumura. Unpublished data.

clinical trial and future phase-II trials of NK012 in patients with advanced solid tumors including RCC might meet or even exceed our expectations.

Acknowledgments

Received 12/10/2007; revised 1/25/2008; accepted 1/31/2008.

Grant support: Grant-in-aid from 3rd Term Comprehensive Control Research for Cancer, Ministry of Health, Labor and Welfare (Y. Matsumura) and Scientific Research on Priority Areas from the Ministry of Education, Culture, Sports, Science and Technology (Y. Matsumura).

The costs of publication of this article were defrayed in part by the payment of page charges. This article must therefore be hereby marked *advertisement* in accordance with 18 U.S.C. Section 1734 solely to indicate this fact.

We thank H. Miyatake and N. Mie for their technical assistance and K. Shiina for her secretarial assistance.

References

1. Matsumura Y, Maeda H. A new concept for macromolecular therapeutics in cancer chemotherapy: mechanism of tumoritropic accumulation of proteins and the antitumor agent smancs. Cancer Res 1986;46:6387–92.
2. Yokoyama M, Miyauchi M, Yamada N, et al. Characterization and anticancer activity of the micelle-forming polymeric anticancer drug adriamycin-conjugated poly(ethylene glycol)-poly(aspartic acid) block copolymer. Cancer Res 1990;50:1693–700.
3. Kataoka K, Harada A, Nagasaki Y. Block copolymer micelles for drug delivery: design, characterization and biological significance. Adv Drug Deliv Rev 2001;47:113–31.
4. Matsumura Y, Hamaguchi T, Ura T, et al. Phase I clinical trial and pharmacokinetic evaluation of NK911, a micelle-encapsulated doxorubicin. Br J Cancer 2004;91:1775–81.
5. Hamaguchi T, Kato K, Yasui H, et al. A phase I and pharmacokinetic study of NK105, a paclitaxel-incorporating micellar nanoparticle formulation. Br J Cancer 2007;97:170–6.
6. Koizumi F, Kitagawa M, Negishi T, et al. Novel SN-38-incorporating polymeric micelles, NK012, eradicate vascular endothelial growth factor-secreting bulky tumors. Cancer Res 2006;66:10048–56.
7. Gasparini G, Harris AL. Clinical importance of the determination of tumor angiogenesis in breast carcinoma: much more than a new prognostic tool. J Clin Oncol 1995;13:765–82.
8. Takahashi Y, Kitadai Y, Bucana CD, Cleary KR, Ellis LM. Expression of vascular endothelial growth factor and its receptor, KDR, correlates with vascularity, metastasis, and proliferation of human colon cancer. Cancer Res 1995;55:3964–8.
9. Williams JK, Carlson GW, Cohen C, Derose PB, Hunter S, Jurkiewicz MJ. Tumor angiogenesis as a prognostic factor in oral cavity tumors. Am J Surg 1994;168:373–80.
10. Natsume T, Watanabe J, Koh Y, et al. Antitumor activity of TZT-1027 (Soblidotin) against vascular endothelial growth factor-secreting human lung cancer *in vivo*. Cancer Sci 2003;94:826–33.
11. Zhang L, Hannay JA, Liu J, et al. Vascular endothelial growth factor overexpression by soft tissue sarcoma cells: implications for tumor growth, metastasis, and chemoresistance. Cancer Res 2006;66:8770–8.
12. Matsumura Y, Maruo K, Kimura M, Yamamoto T, Konno T, Maeda H. Kinin-generating cascade in advanced cancer patients and *in vitro* study. Jpn J Cancer Res 1991;82:732–41.
13. Wu J, Akaike T, Hayashida K, et al. Identification of bradykinin receptors in clinical cancer specimens and murine tumor tissues. Int J Cancer 2002;98:29–35.
14. Maeda H, Fang J, Inutsuka T, Kitamoto Y. Vascular permeability enhancement in solid tumor: various factors, mechanisms involved and its implications. Int Immunopharmacol 2003;3:319–28.
15. Suzuki M, Takahashi T, Sato T. Medial regression and its functional significance in tumor-supplying host arteries. A morphometric study of hepatic arteries in human livers with hepatocellular carcinoma. Cancer 1987;59:444–50.
16. Skinner SA, Tutton PJ, O'Brien PE. Microvascular architecture of experimental colon tumors in the rat. Cancer Res 1990;50:2411–7.
17. An Z, Jiang P, Wang X, Moossa AR, Hoffman RM. Development of a high metastatic orthotopic model of human renal cell carcinoma in nude mice: benefits of fragment implantation compared to cell-suspension injection. Clin Exp Metastasis 1999;17:265–70.
18. Hoffman RM. Orthotopic metastatic mouse models for anticancer drug discovery and evaluation: a bridge to the clinic. Invest New Drugs 1999;17:343–59.
19. Rini BI, Vogelzang NJ, Dumas MC, Wade JL III, Taber DA, Stadler WM. Phase II trial of weekly intravenous gemcitabine with continuous infusion fluorouracil in patients with metastatic renal cell cancer. J Clin Oncol 2000;18:2419–26.
20. Nanus DM, Garino A, Milowsky MI, Larkin M, Dutcher JP. Active chemotherapy for sarcomatoid and rapidly progressing renal cell carcinoma. Cancer 2004;101:1545–51.

Author's personal copy

Journal of Controlled Release 133 (2009) 198–205

Contents lists available at ScienceDirect

Journal of Controlled Release

journal homepage: www.elsevier.com/locate/jconrel

A novel strategy utilizing ultrasound for antigen delivery in dendritic cell-based cancer immunotherapy

Ryo Suzuki [a], Yusuke Oda [a], Naoki Utoguchi [a], Eisuke Namai [a], Yuichiro Taira [a], Naoki Okada [b], Norimitsu Kadowaki [c], Tetsuya Kodama [d], Katsuro Tachibana [e], Kazuo Maruyama [a,*]

[a] Department of Biopharmaceutics, School of Pharmaceutical Sciences, Teikyo University, 1091-1 Suwarashi, Sagamiko-cho, Sagamihara, Kanagawa 229-0195, Japan
[b] Department of Biotechnology and Therapeutics, Graduate School of Pharmaceutical Sciences, Osaka University, 1-6 Yamadaoka, Suita, Osaka 565-0871, Japan
[c] Department of Hematology and Oncology, Graduate School of Medicine, Kyoto University, 54 Shogoin Kawara-cho, Sakyo-ku, Kyoto 606-8507, Japan
[d] Department of Biomedical Engineering, Graduate School of Biomedical Engineering, Tohoku University, 2-1 Seiryo-machi, Aoba-ku, Sendai 980-8575, Japan
[e] Department of anatomy, School of medicine, Fukuoka University, 7-45-1 Nanakuma, Jonan-ku, Fukuoka 814-0180, Japan

ARTICLE INFO

Article history:
Received 12 August 2008
Accepted 16 October 2008
Available online 31 October 2008

Keywords:
Dendritic cells
Antigen delivery system
Cancer immunotherapy
Ultrasound
Liposomes

ABSTRACT

In dendritic cell (DC)-based cancer immunotherapy, it is important that DCs present peptides derived from tumor-associated antigens on MHC class I, and activate tumor-specific cytotoxic T lymphocytes (CTLs). However, MHC class I generally present endogenous antigens expressed in the cytosol. We therefore developed an innovative approach capable of directly delivering exogenous antigens into the cytosol of DCs; i.e., a MHC class I-presenting pathway. In this study, we investigated the effect of antigen delivery using perfluoropropane gas-entrapping liposomes (Bubble liposomes, BLs) and ultrasound (US) exposure on MHC class I presentation levels in DCs, as well as the feasibility of using this antigen delivery system in DC-based cancer immunotherapy. DCs were treated with ovalbumin (OVA) as a model antigen, BLs and US exposure. OVA was directly delivered into the cytosol but not via the endocytosis pathway, and OVA-derived peptides were presented on MHC class I. This result indicates that exogenous antigens can be recognized as endogenous antigens when delivered into the cytosol. Immunization with DCs treated with OVA, BLs and US exposure efficiently induced OVA-specific CTLs and resulted in the complete rejection of E.G7-OVA tumors. These data indicate that the combination of BLs and US exposure is a promising antigen delivery system in DC-based cancer immunotherapy.

© 2008 Elsevier B.V. All rights reserved.

1. Introduction

Dendritic cells (DCs), which are unique antigen-presenting cells capable of priming naive T cells, are promising vaccine carriers for cancer immunotherapy [1]. To induce efficiently a tumor-specific cytotoxic T-lymphocyte (CTL) response, DCs should abundantly present epitope peptides derived from tumor-associated antigens (TAAs) via major histocompatibility complex (MHC) class I molecules [2]. In general, the majority of peptides presented via the MHC class I molecules are generated from endogenously synthesized proteins that are degraded by the proteasome [3]. On the other hand, exogenous antigens such as TAAs for DCs are preferentially presented on MHC class II molecules [3]. In order to prime efficiently TAAs specific for CTLs, it is important to develop a novel antigen delivery system, which can induce MHC class I restricted TAA presentation on DCs. Several researchers are developing antigen delivery tools based on the cross presentation theory of exogenous antigens for DCs [4–8]. In these studies, various types of antigen delivery carriers such as liposomes [6,7], poly(γ-glutamic acid) nanoparticles [5] and cholesterol pullulan nanoparticles [8], all of which can deliver antigen into DCs via the endocytosis pathway, have been developed. We have reported that IgG modified liposomes with entrapped antigen can induce cross presentation of exogenous antigen for DCs on MHC class I molecules [9]. These carriers deliver antigens into DCs via an endocytosis mechanism, with delivery thought to be due to exogenous antigen leaking from the endosome into the cytosol. It is therefore important to design an antigen delivery system which does not rely on the endocytosis pathway. In other study, it was reported that DCs pulsed with exogenous antigens by electroporation presented their antigens on MHC class I molecules and resulted

Abbreviations: Alexa-OVA, Alexa Fluor 488-conjugated ovalbumin; BL, Bubble liposome; CTL, cytotoxic T lymphocyte; DC, dendritic cell; DSPC, 1,2-distearoyl-sn-glycero-phosphatidylcholine; DSPE-PEG(2k)-OMe, 1,2-distearoyl-sn-glycero-3-phosphatidyl-ethanolamine-methoxypolyethyleneglycol; ER, endoplasmic reticulum; FBS, fetal bovine albumin; HLA, human leukocyte antigen; MHC, major histocompatibility complex; MTT, 3-(4,5-s-dimethylthiazol-2-yl)-2,5-diphenyl tetrazolium bromide; NaN_3, sodium azide; OVA, ovalbumin; PBS, phosphate buffer saline; US, ultrasound; TAA, tumor associated antigen.

* Corresponding author. Department of Biopharmaceutics, School of Pharmaceutical Sciences, Teikyo University, 1091-1 Suwarashi, Sagamiko-cho, Sagamihara, Kanagawa 229-0195, Japan. Tel.: +81 42 685 3722; fax: +81 42 685 3432.
E-mail address: maruyama@pharm.teikyo-u.ac.jp (K. Maruyama).

0168-3659/$ – see front matter © 2008 Elsevier B.V. All rights reserved.
doi:10.1016/j.jconrel.2008.10.015

Author's personal copy

in inducing MHC class I-mediated antitumor immunity. Although electroporation is commonly utilized as gene delivery method and deliver gene such as DNA and RNA into cytosol, Kim K.W. et al and Weiss J.M. et al. apply this system to antigen delivery into DCs [10,11]. Their reports also demonstrate the importance of delivering exogenous antigens into cytosol of DCs to induce MHC class I presentation of the antigens.

It has been reported that ultrasound (US) increases the permeability of the plasma membrane, which encourages the entry of DNA into cells [12,13]. The first studies applying US for gene delivery used frequencies in the range of 20–50 kHz [12,14]. However, these frequencies, along with cavitation, are also known to induce tissue damage if not properly controlled [15–17]. To address this problem, many studies into using therapeutic US for gene delivery have used frequencies of 1–3 MHz, intensities of 0.5–2.5 W/cm^2 and a pulse-mode [18–20]. In addition, it was reported that the combination of therapeutic US and microbubble echo contrast agents could enhance gene transfection efficiency [21–27]. In this method, DNA is effectively and directly transferred into the cytosol. This system has been applied to deliver proteins into cells [28,29], but not yet to deliver antigens into DCs for the purpose of cancer immunotherapy. Previously, we developed novel liposomal bubbles containing nanobubbles of the US imaging gas, perfluoropropane [30–34] and suggested that these "Bubble liposomes" (BLs) might be used as novel non-viral gene delivery tools if combined with US exposure. In the case of DCs, the antigen delivered into the cytosol would present on MHC class I molecules and result in priming antigen-specific CTLs. In this study, we examined the effectiveness of BLs combined with US exposure to deliver antigen into DCs. In addition, the effectiveness of this antigen delivery system in DC-based cancer immunotherapy was assessed.

2. Materials and methods

2.1. Cells

T cell hybridoma CD8-OVA1.3 (a kind gift from Dr. C.V. Harding, Department of Pathology, Case Western Reserve University, Cleveland, OH, USA), a cell type that recognizes SIINFEKL:H-2K^b complexes [35], was cultured in Dulbecco's modified Eagle's medium (DMEM, Sigma Chemical Co., St. Louis, MO, USA) supplemented with 10% heat inactivated fetal bovine serum (FBS, GIBCO, Invitrogen Co., Carlsbad, CA, USA), 50 μM 2-mercaptethanol (2-ME), 250 μg/ml amphotericin B (Wako Pure Chemical Industries, Ltd., Osaka, Japan) and 50 μg/ml gentamycin (Wako Pure Chemical Industries). EL-4 murine thymoma cells were cultured in RPMI 1640 supplemented with 10% FBS and 50 μM 2-ME. E.G7-OVA cells (OVA cDNA transfectant of EL4 cells) were maintained in RPMI 1640 supplemented with 10% FBS, 50 μM 2-ME and 400 μg/ml GENETICIN (G418 sulfate, GIBCO, Invitrogen). All culture media contained 50 U/ml penicillin and 50 μg/ml streptomycin (Wako Pure Chemical Industries).

2.2. Generation of mouse bone marrow-derived DCs

DCs were generated from bone marrow cells as described elsewhere [36]. Briefly, bone marrow cells were isolated from C57BL/6 mice and were cultured in RPMI 1640 with 10% FBS, 50 U/ml penicillin, 50 μg/ml streptomycin and 40 ng/ml mouse granulocyte-macrophage colony-stimulating factor (GM-CSF). After 8–16 days of culture, non-adherent cells were collected and used as DCs.

2.3. Preparation of BLs

Liposomes composed of 1,2-distearoyl-sn-glycero-phosphatidylcholine (DSPC) (NOF Corp., Tokyo, Japan) and 1,2-distearoyl-sn-glycero-3-phosphatidyl-ethanolamine-methoxypolyethyleneglycol (DSPE-PEG(2k)-OMe, (PEG Mw=ca. 2000), NOF) (94 : 6 (m/m)) were prepared by reverse phase evaporation. Briefly, all reagents (total lipid: 100 μmol) were dissolved in 8 ml of 1:1 (v/v) chloroform/diisopropyl ether, then 4 ml of phosphate buffered saline (PBS) was added. The mixture was sonicated and evaporated at 65 °C. The solvent was completely removed, and the size of the liposomes was adjusted to less than 200 nm using an extruding apparatus (Northern Lipids Inc., Vancouver, BC, Canada) and sizing filters (pore sizes: 100 and 200 nm; Nuclepore Track-Etch Membrane, Whatman plc, UK). After sizing, the liposomes were sterilized by passing them through a 0.45 μm pore size filter (MILLEX HV filter unit, Durapore PVDF membrane, Millipore Corp., MA, USA). The size of the liposomes was measured by dynamic light scattering (ELS-800, Otsuka Electronics Co., Ltd., Osaka, Japan). The average diameter of these liposomes was between 150–200 nm. Lipid concentration was measured using the Phospholipid C test (Wako Pure Chemical Industries). BLs were prepared from the liposomes and perfluoropropane gas (Takachiho Chemical Industrial Co., Ltd., Tokyo, Japan) [31,33]. Briefly, 5 ml sterilized vials containing 2 ml of the liposome suspension (lipid concentration: 2 mg/ml) were filled with perfluoropropane, capped, and then supercharged with 7.5 ml of perfluoropropane. The vial was placed in a bath-type sonicator (42 kHz, 100 W; BRANSONIC 2510J-DTH, Branson Ultrasonics Co., Danbury, CT, USA) for 5 min to form the BLs. In this method, the liposomes were reconstituted by sonication under the condition of supercharge with perfluoropropane in the 5 mL vial container. At the same time, perfluoropropane would be entrapped within lipids like micelles, which were made by DSPC and DSPE-PEG(2k)-OMe from liposome composition, to form nanobubbles. The lipid nanobubbles were encapsulated within the reconstituted liposomes, which sizes were changed into around 1 μm from 150–200 nm of original.

2.4. Antigen trafficking into DCs after antigen delivery with BLs and US exposure

Alexa Fluor 488 conjugated OVA (Alexa-OVA) was prepared with Alexa Fluor 488 succinimidyl ester (Molecular Probes, Invitrogen) according to the instruction manual. DCs (1×10^5 cells/ml) were cultured in a glass bottom dish (IWAKI, Asahi Glass Co. Ltd., Tokyo, Japan) overnight. After washing the cells with OptiMEM (Invitrogen), BLs (240 μg/ml) and Alexa-OVA (50 μg/ml) were added to the dish. Then, the DCs were exposed to US exposure (frequency: 2 MHz, duty: 10%, burst rate: 2.0 Hz, intensity 2.0 W/cm^2, time: 3×10 s (interval: 10 s)) using a Sonopore 4000 (6 mm diameter probe; Nepa Gene Co. Ltd., Chiba, Japan). This condition was decided referring to our reports about gene delivery [31,33] and Guo et al.'s report about the repeat US exposure with interval [37], and from the viewpoint of cytotoxicity for DCs. After US exposure, the DCs were incubated for 1 h at 37 °C, then washed with PBS, fixed with 3% paraformaldehyde for 10 min, and treated with 0.1% Triton X-100 (Wako Pure Chemical Industries) for 5 min. In addition, some DCs were washed with PBS, their nuclei were stained with propidium iodide (0.5 μg/ml) (Wako Pure Chemical Industries), and antigen trafficking was observed with a confocal laser microscope.

2.5. Antigen delivery following inhibition of the endocytosis pathway in DCs

DCs were pretreated with OptiMEM containing 10 mM NaN_3 for 1 h at 4 °C to inhibit the endocytosis pathway. After washing the cells, BLs (240 μg/ml) and Alexa-OVA (50 μg/ml) were added to the DCs in OptiMEM containing 10 mM sodium azide (NaN_3). The DCs were exposed to US exposure (frequency: 2 MHz, duty: 10%, burst rate: 2.0 Hz, intensity 2.0 W/cm^2, time: 3×10 s (interval: 10 s)), then washed with PBS containing10 mM NaN_3. After US exposure, DCs were fixed and their nuclei were stained as described above (2.4.).

Author's personal copy

2.6. Flow cytometry analysis of antigen delivery into DCs with BLs and US exposure

Alexa-OVA was delivered into DCs under inhibited endocytosis conditions as described above (2.5.). After washing, the DCs were stained with propidium iodide (100 ng/ml) and analyzed by flow cytometry (FACSCalibur, Becton, Dickinson and Company, Franklin Lakes, NJ, USA). In this study, living DCs (1×10^4 cells) were analyzed by gating out propidium iodide staining cells.

2.7. Assessment of MHC class I restricted OVA presentation

DCs (2.5×10^5 cells/500 μl/well (48-well plate)) were pulsed with OVA alone (0, 10, 100, 1000 μg/ml) or OVA (0, 10, 100, 1000 μg/ml) using US exposure (frequency: 2 MHz, duty: 10%, burst rate: 2.0 Hz, intensity 2.0 W/cm^2, Time: 3×10 s (interval: 10 s)) and/or BLs (240 μg/ml). After US exposure, the DCs were incubated for 1 h at 37 °C, then washed with PBS. After culturing for 24 h, the DCs were co-cultured for 20 h with T cell hybridoma CD8-OVA1.3 (2×10^5 cells/well) that recognizes SIINFEKL: H-2K^b complexes. The concentration of IL-2 in the supernatants was measured using an IL-2 ELISA Kit (BioSource International, Inc., Camarillo, CA, USA).

2.8. Assessment of cytotoxicity to DCs by the treatment of BLs and US exposure

DCs (2.5×10^5 cells/500 μl/well (48-well plate)) were treated with BLs (240 μg/ml) and/or US exposure (frequency: 2 MHz, duty: 10%, burst rate: 2.0 Hz, intensity 2.0 W/cm^2, Time: 3×10 s (interval: 10 s)). After US exposure, DCs were incubated for 1 h at 37 °C, and washed with PBS. The DCs were resuspended with cuture medium (250 μl) and cultured for 48 h. Cell viability was assayed using MTT (3-(4,5-s-dimethylthiazol-2-yl)-2,5-diphenyl tetrazolium bromide, Dojindo, Kumamoto, Japan) as described by Mosmann with minor modifications [38]. Briefly, MTT (5 mg/mL, 25 μL) was added to each well and the cells were incubated at 37 °C for 4 h. The formazan product was dissolved in 250 μL of 10% sodium dodecyl sulfate (SDS, Wako Pure Chemical Ind. Co., Ltd. Osaka, Japan) containing 15 mM HCl. Color intensity was measured using a microplate reader (POWERSCAN HT; Dainippon Pharmaceutical, Osaka, Japan) at test and reference wavelengths of 595 and 655 nm, respectively.

2.9. Immunization of mice with DCs and cytotoxicity assay

DCs (2.5×10^5 cells/500 μl/well) were pulsed with OVA alone (100 μg/ml) or OVA (100 μg/ml) using US exposure (frequency: 2 MHz, duty: 10%, burst rate: 2.0 Hz, intensity 2.0 W/cm^2, Time: 3×10 s (interval: 10 s)) and/or BLs (240 μg/ml) on a 48-well plate, then collected from 10 wells and seeded into 6-well plates. After 1 h incubation at 37 °C, the DCs were washed and cultured for 24 h at 37 °C. After washing, DCs (1×10^6 cells/100 μl) were intradermally injected into the backs of C57BL/6 mice. After 7 days, the mice were re-immunized. Seven days after the second immunization, splenocytes were obtained from five mice, and the splenocytes were pooled and stimulated with mitomycin C-treated E.G7-OVA cells at a ratio of 10:1 for 5 days. The stimulated splenocytes were used as effector cells for the cytotoxicity assay, using EL-4 or E.G7-OVA as the target cells in a flow cytometric assay employing two fluorochromes [39]. PKH-67, a fluorochrome which fluoresces green, binds to the cytoplasmic membrane and does not leak or transfer, was used to identify the target cell population. Propidium iodide fluoresces red and was used to detect non-viable cells. Use of these two fluorochromes and two parameter analyses allowed the identification of four subpopulations in the sample: live effectors, dead effectors, live targets and dead targets. By enumerating these subpopulations, the percent target lysis can be calculated.

2.10. Antitumor effect by prior immunization with antigen-pulsed DCs

DCs (2.5×10^5 cells/500 μl/well) were pulsed with OVA alone (100 μg/ml) or OVA (100 μg/ml) using US exposure (frequency: 2 MHz, duty: 10%, burst rate: 2.0 Hz, intensity 2.0 W/cm^2, Time: 3×10 s (interval: 10 s)) and/or BLs (240 μg/ml) on a 48-well plate, then collected from 10 wells and seeded into 6-well plates. After 1 h incubation at 37 °C, the DCs were washed and cultured for 24 h at 37 °C. After washing, the DCs (1×10^6 cells/100 μl) were intradermally immunized into the backs of C57BL/6 mice twice at intervals of one week. Seven days after the second immunization, E.G7-OVA cells (1×10^6 cells) were intradermally inoculated into the backs of mice and the size of the tumors was monitored using the formula: (major axis×minor axis^2)×0.5. All treated groups contained five mice.

2.11. Re-challenge of tumor cells

E.G7-OVA cells (1×10^6 cells) were injected into mice that were resistant to tumor cells due to immunization with DCs treated with BLs, US exposure and OVA. Untreated mice were used as controls to confirm the development of cancer following the first inoculation with E.G7-OVA cells. All treated groups contained five mice.

2.12. Treatment of tumor-bearing mice with antigen-pulsed DCs

E.G7-OVA cells (1×10^6 cells) were intradermally inoculated into the backs of C57BL/6 mice. On day 9, when the tumors were between 8–10 mm, OVA pulsed DCs (1×10^6 cells) prepared as described above were intradermally injected into the backs of the mice. On day 12, DCs were injected similarly. Tumor sizes were monitored from the day of inoculation. All treated groups contained five mice.

2.13. Statistical analysis

Differences in IL-2 secretion between the experimental groups were compared using non-repeated measures ANOVA and Dunnett's test.

3. Results

3.1. Antigen delivery by BLs and sonoporation into the cytosol of DCs lacking the endocytosis pathway

We examined antigen trafficking following delivery using a combination of BLs and US exposure (Fig. 1(a)). In DCs treated with Alexa-OVA in the presence or absence of either BLs or US exposure, the fluorescence from Alexa-OVA appeared as dots in the cytosol. On the other hand, in DCs treated with Alexa-OVA, BLs and US exposure, the fluorescence appeared as dots, but also as diffused fluorescence in the cytosol. To confirm this, antigen delivery was examined following inhibition of the endocytosis pathway in DCs by treatment with sodium azide (Fig. 1(b)). In DCs treated with Alexa-OVA either with or without BLs or US exposure, the fluorescence derived from Alexa-OVA was not observed. On the other hand, in DCs treated with Alexa-OVA, BLs and US exposure, fluorescence was observed in the cytosol even when the endocytosis pathway in DCs was inhibited. In addition, the efficiency of antigen delivery following inhibition of the endocytosis pathway was assessed using flow cytometory (Fig. 1(c)). The fluorescence intensity of DCs treated with Alexa-OVA, BLs and US exposure was higher than that of DCs treated with Alexa-OVA alone, or of Alexa-OVA and BLs or US exposure. These data support the data shown in Fig. 1(b), indicating that Alexa-OVA is observed in the cytosol when DCs are only treated with BLs and US exposure, even when the endocytosis pathway is

Author's personal copy

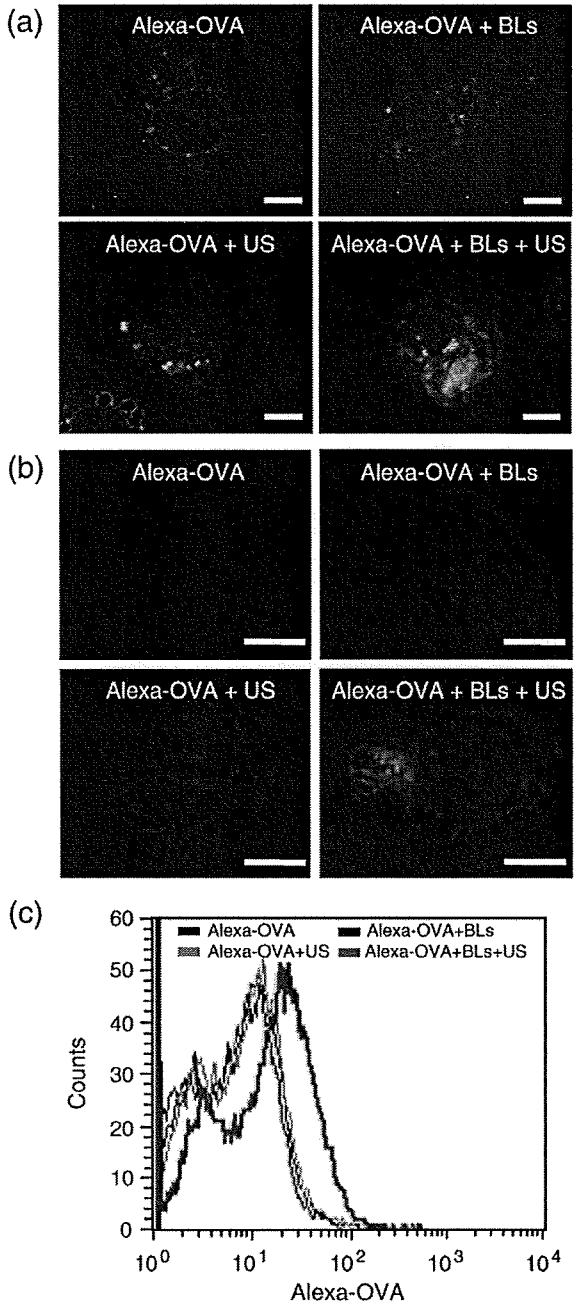

Fig. 1. Intracellular antigen delivery into DCs using BLs and US exposure. (a) Uptake of Alexa-OVA into DCs. DCs were cultured in a glass bottom dish overnight. After washing the cells, Alexa-OVA was added to the dish. Then, the DCs were exposed to US in the presence or absence of BLs and incubated for 1 h at 37 °C. The DCs were washed with PBS, fixed, and the nuclei were stained with propidium iodide. The uptake of Alexa-OVA was observed using a confocal laser microscope. (b) Intracellular delivery of Alexa-OVA into DCs using BLs and US. DCs were pretreated with OptiMEM containing 10 mM NaN_3 for 1 h at 4 °C to inhibit the endocytosis pathway. After washing the cells, Alexa-OVA was added to the DCs in OptiMEM containing10 mM NaN_3. Then, the DCs were exposed to US in the presence or absence of BLs. After US exposure, the DCs were washed with PBS containing 10 mM NaN_3, fixed, and the nuclei were stained with propidium iodide. Intracellular trafficking of Alexa-OVA in the DCs was observed using a confocal laser microscope. Scale bar shows 5 μm. (c) Flow cytometry analysis of DCs containing Alexa-OVA delivered using BLs and US. Alexa-OVA was delivered into the cell interior of the DCs during endocytosis inhibition. After washing the cells, the DCs were analyzed by flow cytometry.

inhibited. These results suggest that the combination of BLs and US exposure can be used to directly deliver antigens into the cytosol of DCs in the absence of endocytosis.

3.2. MHC class I presentation of exogenous antigen delivered into DCs by BLs and US exposure

Exogenous antigen delivered into the cytosol of DCs by BLs and US exposure is recognized as endogenous antigen by DCs and leads to the efficient presentation of peptides derived from exogenous antigens on MHC class I molecules. Thus, we examined whether antigen delivery by BLs and US exposure resulted in the efficient presentation of peptides on MHC class I molecules and the stimulation of $CD8^+$ T cells. C57BL/6-derived OVA-specific T cell hybridoma CD8-OVA1.3 was co-cultured with mouse bone marrow-derived DCs pulsed with antigen. As shown in Fig. 2, CD8-OVA1.3 cells stimulated with DCs pulsed with soluble OVA, either treated or untreated by BLs or US exposure did not secrete a significant amount of IL-2. Of note, a larger amount of IL-2 was secreted by CD8-OVA1.3 cells stimulated with DCs pulsed with OVA treated with a combination of BLs and US exposure. These data indicate that antigen delivery by BLs to DCs upon sonoporation results in the presentation of peptides derived from OVA on MHC class I molecules. In this data, the level of IL-2 secretion increased depending on OVA concentration and reached plateau in 100 μg/ml of OVA concentration. Therefore, we used this OVA concentration (100 μg/ml) in further examinations.

3.3. Cytotoxicity to DCs by the treatment of BLs and US exposure

In this antigen delivery system using BLs and US exposure, the transient pores would be provided on the membrane of DCs. Therefore, it is concerned that the DCs are injured by US exposure in the presence of BLs. To assess the cytotoxicity to DCs by the treatment of BLs and US exposure, we examined about the viability of DCs (Fig. 3). In the treatment of DC with BLs and/or US exposure, the viability of DCs treated with BLs, US exposure or BLs/US exposure was 83 ± 11%, 96 ± 5% or 87 ± 13%, respectively. This result shows that there is not serious damage to DCs even under the condition of inducing transient pores on the membrane of DCs treated with BLs and US exposure.

3.4. Induction of antigen-specific CTL response in the immunization of DCs pulsed with antigen using BLs and US exposure

To examine whether efficient peptide presentation on MHC class I molecules leads to strong induction of antigen-specific CTLs *in vivo*, we immunized C57BL/6 mice twice with bone marrow-derived DCs that had been treated with various antigen delivery techniques. Thereafter, splenocytes were isolated, and a cytotoxicity assay was

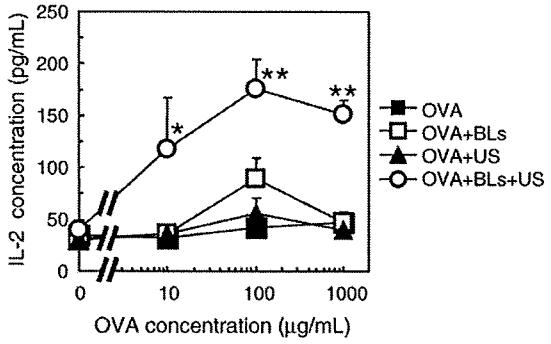

Fig. 2. MHC class I restricted OVA presentation after OVA delivery into DCs using a combination of BLs and US exposure. DCs were pulsed with OVA alone or OVA in conjunction with US exposure and/or BLs. After US exposure, the DCs were incubated for 1 h at 37 °C, then washed with PBS. After culturing for 24 h, the DCs were co-cultured with CD8-OVA1.3 cells for 20 h. The concentration of IL-2 in the supernatants was measured. Each data represents the mean ± S.D. for triplicate measurements. *$P<0.05$ compared to the group treated with BLs or US, or without BLs and US. **$P<0.01$ compared to the group treated with BLs or US, or without BLs and US.

Author's personal copy

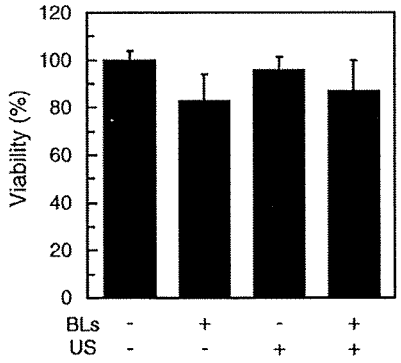

Fig. 3. Viability of DCs treated with BLs and /or US exposure. DCs were treated with BLs and/or US. After US exposure, DCs were incubated for 1 h at 37 °C, then washed with PBS. After culturing for 48 h, the viability of DCs was measured by MTT assay. Each data represents the mean ± S.D. for triplicate measurements.

performed using the syngeneic lymphoma cell line EL-4 or its OVA transfectant, E.G7-OVA. As shown in Fig. 4, immunization with DCs without OVA, DCs pulsed with OVA, or OVA combined with BLs or US exposure, induced weak cytotoxicity of splenocytes against the OVA-expressing cell line E.G7-OVA. In contrast, immunization with DCs pulsed with OVA following BL and US exposure resulted in strong cytotoxicity against the OVA-expressing cell line E.G7-OVA by splenocytes. Splenocytes from mice immunized with DCs pulsed using any method of antigen delivery did not exhibit strong cytotoxicity against the parental cell line EL-4. These data indicate that DCs pulsed with antigen using BLs and US exposure as the antigen delivery method efficiently present peptides on MHC class I molecules, which results in strong induction of antigen-specific CTLs *in vivo*.

3.5. Antitumor effects in the immunization of DCs pulsed with antigen by BLs and US exposure

Using an E.G7-OVA tumor model, we examined whether the strong induction of CTLs by antigen delivery with BLs and US exposure leads to efficient anti-tumor immune responses *in vivo*. We immunized C57BL/6 mice twice with bone marrow-derived DCs that had been pulsed using one of two methods of antigen delivery (OVA with US exposure, or OVA with BLs and US exposure). One week after the second immunization, the mice were inoculated intradermally with E.G7-OVA cells, and tumor growth was monitored. As shown in Fig. 5(a) and (b), immunization with untreated DCs weakly suppressed tumor growth. The survival rate of mice immunized with untreated DCs was slightly prolonged, suggesting that non-specific inflammatory responses induced by the injection of DCs result in weak anti-tumor immune responses. Immunization with DCs that had been pulsed with OVA using US exposure suppressed tumor growth slightly more efficiently than the control immunization. Of note, immunization with DCs that had been pulsed with OVA using BLs and US exposure completely suppressed tumor growth, with all mice in this group surviving more than 70 days after tumor inoculation. In addition, we examined the prevention of tumor growth recurrence after re-inoculation of tumor cells into mice, which had completely rejected the first injection of tumor cells (Fig. 5(c)). All mice, which were re-inoculated with E.G7-OVA cells 10 weeks after the first inoculation, completely rejected the tumor cells.

Finally, we examined whether immunization with DCs pulsed with antigen using BLs and US exposure can efficiently suppress the growth of established tumors. For this purpose, we inoculated C57BL/6 mice with E.G7-OVA, and after 9 and 12 days, when the tumors were between 100–200 mm^3, DCs were injected intradermally. As shown in Fig. 6(a), administration of untreated DCs did not provide a significant therapeutic effect. Administration of DCs pulsed with OVA using US exposure exhibited a weak therapeutic effect. Importantly, administration of DCs pulsed with OVA using BLs and US exposure exhibited stronger therapeutic effects in two of the five mice, with these two mice surviving for more than 60 days (Fig. 6(b)). These data indicate that antigen delivery into DCs with BLs and US exposure can induce significant therapeutic effects on established tumors.

4. Discussion

Subunit vaccines utilizing MHC class I-binding peptides have significant limitations that hinder their application to the general patient population (restrictions of HLA types) and that also affect their clinical effectiveness (monovalency of tumor specific antigen) in DC-based tumor immunotherapy. Utilization of tumor associated proteins as antigens may overcome this limitation, thereby enabling a broad spectrum of peptide presentation. In fact, patients treated with tumor cell lysates pulsed DCs showed better response rates compared with patients treated with peptide pulsed DCs [40]. This clinical trial suggests that tumor lysates are a good source of tumor antigens for a polyvalent antitumor vaccine. On the other hand, MHC class I molecules generally present endogenous antigens, whereas exogenous antigens for DCs are taken up by the endocytosis pathway and exogenous antigen-derived peptides are presented on MHC class II molecules [3]. In this study, we showed that by using a combination of BLs and US exposure, exogenous antigen was directly delivered into the cytosol of DCs (Fig. 1) and was presented on MHC class I molecules (Fig. 2). In addition, DCs immunized with antigen delivered by BLs and US exposure could stimulate antigen-specific CTL activation (Fig. 4) and resulted in inducing effective anti-tumor immune responses in tumor-bearing mice. (Figs. 5 and 6) Although peptide and protein delivery with sonoporation using microbubbles have been previously reported [28,29,41], the present study is the first report of effective antigen delivery into DCs by BLs using sonoporation for cancer immunotherapy.

Sonoporation and microbubbles such as Optison have been reported to be an effective gene delivery method using non-viral vectors. In addition, peptide and protein delivery with microbubbles and US exposure has been reported [28,29,41]. In the reports, Bekeredjian et al. showed the feasibility of microbubbles and US exposure for delivery of bioactive protein (luciferase, 60 kDa) into the cytosol of *in vitro* and *in vivo* cells [28,29]. Larina I.V. et al. reported that FITC-dextrans of 10–2000 kDa were delivered into human breast

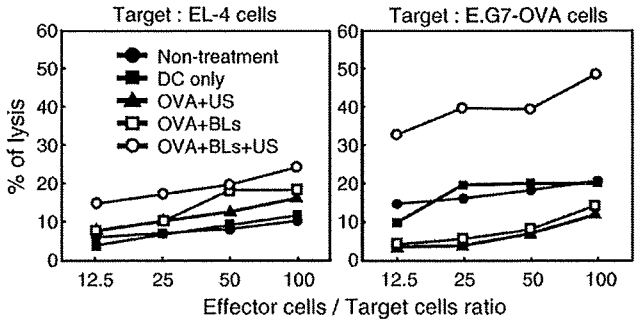

Fig. 4. Antigen specific CTL induction after immunization with DCs treated with BLs and US exposure. DCs were pulsed with OVA under each condition and cultured. After washing the cells, the DCs were intradermally injected into the backs of C57BL/6 mice. After 7 days, the mice were re-immunized. Seven days after the second immunization, splenocytes were obtained and stimulated with mitomycin C-treated E.G7-OVA cells at a ratio of 10:1 for 5 days. The stimulated splenocytes were used as effector cells for a cytotoxicity assay, using EL-4 or E.G7-OVA cells as the target in a flow cytometric assay.

Author's personal copy

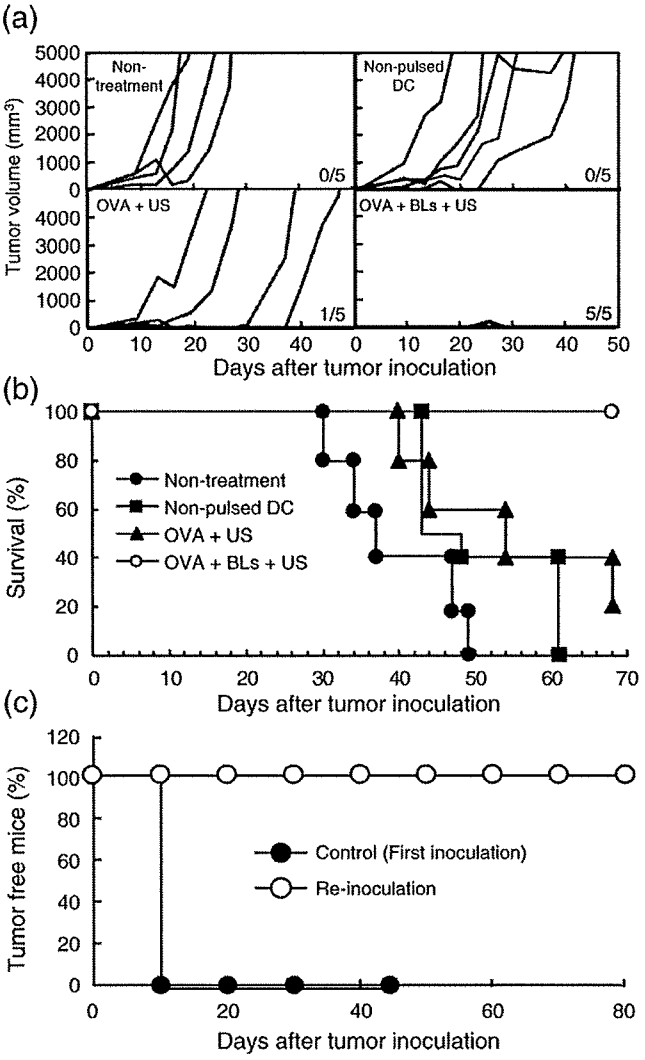

Fig. 5. Antitumor effect caused by immunization of DCs treated with antigen, BLs and US exposure. C57BL/6 mice were immunized with DCs twice. Seven days after the second immunization, E.G7-OVA cells were intradermally inoculated into the backs of the mice, and the tumor volume and survival of the mice was monitored. (a): Tumor volume of the mice after tumor inoculation. Each line indicates the tumor volume in an individual mouse. The fractional number in the lower right of each group shows the number of mice completely rejecting tumors / the number of total experimental mice. (b): Survival rate of the mice after tumor inoculation. (c): Tumor rejection efficiency after re-inoculation with tumor cells. E.G7-OVA cells were re-injected into the mice, which had rejected tumor cells following immunization with DCs treated with OVA, BLs and US in a prior immunization (a). Normal mice were used as controls to confirm the development of cancer following the first inoculation with E.G7-OVA cells. All treated groups contained five mice.

adenocarcinoma (MCF7) by the combination of Optison (conventional microbubbles) and US exposure [42]. It is believed that the delivery mechanism is due to the presence of transient pores through the cell membrane, resulting in extracellular molecules being directly delivered into the cytosol [22,43]. As shown in Fig. 1(b), antigen was directly delivered into DCs by the combination of BLs and US exposure even when the endocytosis pathway was inhibited. Therefore, it is thought that the antigen delivery mechanism induced by BLs and sonoporation is the same as that induced by microbubbles and sonoporation. In studies using microbubbles and sonoporation, pore sizes (based on the physical diameter of the component compounds) were typically between 30–100 nm, and estimates of the membrane recovery time ranged from a few seconds to a few minutes [44]. On the other hand, in studies on the aftereffects of US exposure on cell membranes, Eshet *et al.* reported that microbubbles resulted in a rougher cell surface characterized by depressions, but that the effects are reversible within 24 h following US exposure [43]. In the present study, DCs were incubated with antigen for 1 h after US exposure and increased the delivery efficiency of antigen into the cytosol of DCs. We confirmed the efficiency of MHC class I antigen presentation in DCs with/without 1 h incubation after US exposure. The efficiency following 1 h incubation was higher than that without incubation (data not shown). This result suggests that the membrane permeability of DCs increases even after US exposure. Although the mechanism behind antigen delivery by BLs is unknown, our data support a temporary increase in permeability of the plasma membrane after US exposure. Moreover, recent data from microbubble studies suggest that the resealing of US-induced pores is an energy-dependent process, with the cells exhibiting morphological features consistent with an active and vesicle-based wound-healing responses [45]. Therefore, cells treated with sonoporation are viable due to this recovery mechanism. In this study, the viability of the DCs treated with BLs and US exposure was maintained more than 85% (Fig. 3). The accumulated evidence suggests that the combination of BLs and US exposure is an unique antigen delivery system which can deliver exogenous antigens into the cytosol without serious damage to DCs.

In this study, exogenous antigens, directly delivered into the cytosol of DCs by means of BLs and US exposure, were presented on MHC class I molecules. In addition, immunization of DCs treated with antigen, BLs and US exposure effectively primed antigen-specific CTLs. On the other hand, MHC class I antigen presentation lead to low-level

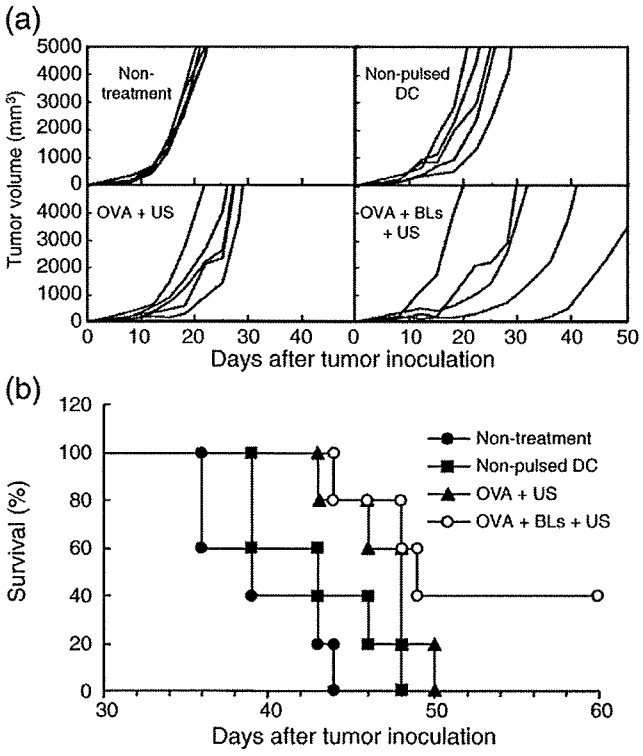

Fig. 6. Immunization of DCs treated with antigen, BLs and US exposure: therapeutic effect on tumor growth. E.G7-OVA cells were intradermally inoculated into the backs of C57BL/6 mice. On day 9, at a tumor size of 8–10 mm, OVA pulsed DCs were intradermally injected into the backs of the mice. On day 12, DCs were injected similarly. The tumor volume and survival of the mice was monitored. (a): Tumor volume of the mice after tumor inoculation. Each line indicates the tumor volume in individual mice. (b): Survival rate of the mice after tumor inoculation. All treated groups contained five mice.

Author's personal copy

antigen delivery with either BLs or US exposure. In these treated cells, antigen was mainly taken up via the endocytosis pathway. Although we have not confirmed MHC class II presentation, the antigen would presumably be presented on MHC class II molecules to DCs via the general antigen processing mechanism [10]. The exogenous antigens directly delivered into the cytosol would be processed similarly endogenously derived antigens, which are enzymatically digested into peptides, mainly by cytosolic proteases called proteasomes, and are then transported by transporters associated with antigen processing (TAP) molecules into the endoplasmic reticulum (ER). In the ER lumen, peptides bind to MHC class I molecules, which are subsequently transported via the Golgi apparatus to the cell surface [46]. Moreover, immunization of DCs treated with OVA, BLs and US exposure could prime OVA-specific CTLs. This result indicates that DCs presented with OVA-derived epitope peptides on MHC class I molecules effectively prime OVA-specific CTLs *in vivo*. We suspected that the effective priming of antigen-specific CTLs would result in the rejection of tumor cells. As shown in Fig. 5(a), all the immunized mice completely rejected the inoculated tumor cells. Tumor cells were intradermally re-injected into these mice to re-challenge their immune system and assess the preventive effects of immunization for suppressing tumor regeneration (Fig. 5(c)). Rejection following re-challenge with tumor cells suggests the induction of an antigen memory system in the host's immune system, i.e., memory T cells for the immunization antigen. Thus, this therapeutic method has potential for suppressing the regeneration and metastasis of tumors. Finally, we also assessed the therapeutic effects of this treatment towards established tumors (Fig. 6). Immunization with DCs treated with antigen, BLs and US exposure lead to significant therapeutic effects towards established tumors. Tumor cells generally secrete cytokines such as TGF-β to suppress the host's immune system. It is therefore possible that antigen delivery with BLs and US exposure could effectively induce an anti-tumor immune response even in the presence of established tumors.

In conclusion, we have developed a novel system for delivering antigens into DCs using BLs and sonoporation. Immunization of DCs using this antigen delivery system could effectively prime the anti-tumor immune system due to the induction of MHC class I TAA presentation. Therefore, BLs in conjunction with sonoporation might be a useful antigen delivery system for DC-based cancer immunotherapy. In the future, this system will be applied to various antigens containing unknown TAAs, such as crude antigens separated from surgically-removed human tumors.

Acknowledgments

The authors thank Mr. Shota Otake, Mr. Norihito Nishiie, Mr. Ken Osawa, Ms. Risa Koshima, Ms. Motoka Kawamura, Mr. Ryo Tanakadate, Mr. Kunihiko Matsuo and Mr. Yasuyuki Shiono (Teikyo University) for their technical assistance, and Mr. Yasuhiko Hayakawa, Mr. Takahiro Yamauchi and Mr. Kosho Suzuki (Nepa Gene Co., Ltd.) for their technical advice regarding US exposure. This study was supported by the Program for Promotion of Fundamental Studies in Health Sciences of the National Institute of Biomedical Innovation (NIBIO). Tetsuya Kodama acknowledges the Grant for Research on Nanotechnical Medical, the Ministry of Health, Labour and Welfare of Japan (H19-nano-010).

References

[1] F.O. Nestle, A. Farkas, C. Conrad, Dendritic-cell-based therapeutic vaccination against cancer, Curr. Opin. Immunol. 17 (2005) 163–169.
[2] J. Copier, A. Dalgleish, Overview of tumor cell-based vaccines, Int. Rev. Immunol. 25 (2006) 297–319.
[3] R.N. Germain, MHC-dependent antigen processing and peptide presentation: providing ligands for T lymphocyte activation, Cell 76 (1994) 287–299.
[4] P. Elamanchili, M. Diwan, M. Cao, J. Samuel, Characterization of poly(D,L-lactic-co-glycolic acid) based nanoparticulate system for enhanced delivery of antigens to dendritic cells, Vaccine 22 (2004) 2406–2412.
[5] T. Yoshikawa, N. Okada, A. Oda, K. Matsuo, K. Matsuo, Y. Mukai, Y. Yoshioka, T. Akagi, M. Akashi, S. Nakagawa, Development of amphiphilic gamma-PGA-nanoparticle based tumor vaccine: potential of the nanoparticulate cytosolic protein delivery carrier, Biochem. Biophys. Res. Commun. 366 (2008) 408–413.
[6] P. Machy, K. Serre, L. Leserman, Class I-restricted presentation of exogenous antigen acquired by Fcgamma receptor-mediated endocytosis is regulated in dendritic cells, Eur. J. Immunol. 30 (2000) 848–857.
[7] N. Okada, T. Saito, K. Mori, Y. Masunaga, Y. Fujii, J. Fujita, K. Fujimoto, T. Nakanishi, K. Tanaka, S. Nakagawa, T. Mayumi, T. Fujita, A. Yamamoto, Effects of lipofectin-antigen complexes on major histocompatibility complex class I-restricted antigen presentation pathway in murine dendritic cells and on dendritic cell maturation, Biochim. Biophys. Acta 1527 (2001) 97–101.
[8] L. Wang, H. Ikeda, Y. Ikuta, M. Schmitt, Y. Miyahara, Y. Takahashi, X. Gu, Y. Nagata, Y. Sasaki, K. Akiyoshi, J. Sunamoto, H. Nakamura, K. Kuribayashi, H. Shiku, Bone marrow-derived dendritic cells incorporate and process hydrophobized polysaccharide/oncoprotein complex as antigen presenting cells, Int. J. Oncol. 14 (1999) 695–701.
[9] K. Kawamura, N. Kadowaki, R. Suzuki, S. Udagawa, S. Kasaoka, N. Utoguchi, T. Kitawaki, N. Sugimoto, N. Okada, K. Maruyama, T. Uchiyama, Dendritic cells that endocytosed antigen-containing IgG-liposomes elicit effective antitumor immunity, J. Immunother. 29 (2006) 165–174.
[10] K.W. Kim, S.H. Kim, J.H. Jang, E.Y. Lee, S.W. Park, J.H. Um, Y.J. Lee, C.H. Lee, S. Yoon, S.Y. Seo, M.H. Jeong, S.T. Lee, B.S. Chung, C.D. Kang, Dendritic cells loaded with exogenous antigen by electroporation can enhance MHC class I-mediated antitumor immunity, Cancer Immunol. Immunother. 53 (2004) 315–322.
[11] J.M. Weiss, C. Allen, R. Shivakumar, S. Feller, L.H. Li, L.N. Liu, Efficient responses in a murine renal tumor model by electroloading dendritic cells with whole-tumor lysate, J. Immunother. 28 (2005) 542–550.
[12] M. Fechheimer, J.F. Boylan, S. Parker, J.E. Sisken, G.L. Patel, S.G. Zimmer, Transfection of mammalian cells with plasmid DNA by scrape loading and sonication loading, Proc. Natl. Acad. Sci. U. S. A. 84 (1987) 8463–8467.
[13] M.W. Miller, D.L. Miller, A.A. Brayman, A review of in vitro bioeffects of inertial ultrasonic cavitation from a mechanistic perspective, Ultrasound Med. Biol. 22 (1996) 1131–1154.
[14] M. Joersbo, J. Brunstedt, Protein synthesis stimulated in sonicated sugar beet cells and protoplasts, Ultrasound Med. Biol. 16 (1990) 719–724.
[15] D.L. Miller, S.V. Pislaru, J.E. Greenleaf, Sonoporation: mechanical DNA delivery by ultrasonic cavitation, Somat. Cell Mol. Genet. 27 (2002) 115–134.
[16] H.R. Guzman, A.J. McNamara, D.X. Nguyen, M.R. Prausnitz, Bioeffects caused by changes in acoustic cavitation bubble density and cell concentration: a unified explanation based on cell-to-bubble ratio and blast radius, Ultrasound Med. Biol. 29 (2003) 1211–1222.
[17] W. Wei, B. Zheng-zhong, W. Yong-jie, Z. Qing-wu, M. Ya-lin, Bioeffects of low-frequency ultrasonic gene delivery and safety on cell membrane permeability control, J. Ultrasound Med. 23 (2004) 1569–1582.
[18] H.J. Kim, J.F. Greenleaf, R.R. Kinnick, J.T. Bronk, M.E. Bolander, Ultrasound-mediated transfection of mammalian cells, Hum. Gene Ther. 7 (1996) 1339–1346.
[19] D.B. Tata, F. Dunn, D.J. Tindall, Selective clinical ultrasound signals mediate differential gene transfer and expression in two human prostate cancer cell lines: LnCap and PC-3, Biochem. Biophys. Res. Commun. 234 (1997) 64–67.
[20] M. Duvshani-Eshet, M. Machluf, Therapeutic ultrasound optimization for gene delivery: a key factor achieving nuclear DNA localization, J. Control. Release 108 (2005) 513–528.
[21] W.J. Greenleaf, M.E. Bolander, G. Sarkar, M.B. Goldring, J.F. Greenleaf, Artificial cavitation nuclei significantly enhance acoustically induced cell transfection, Ultrasound Med. Biol. 24 (1998) 587–595.
[22] Y. Taniyama, K. Tachibana, K. Hiraoka, M. Aoki, S. Yamamoto, K. Matsumoto, T. Nakamura, T. Ogihara, Y. Kaneda, R. Morishita, Development of safe and efficient novel nonviral gene transfer using ultrasound: enhancement of transfection efficiency of naked plasmid DNA in skeletal muscle, Gene Ther. 9 (2002) 372–380.
[23] S. Chen, J.H. Ding, R. Bekeredjian, B.Z. Yang, R.V. Shohet, S.A. Johnston, H.E. Hohmeier, C.B. Newgard, P.A. Grayburn, Efficient gene delivery to pancreatic islets with ultrasonic microbubble destruction technology, Proc. Natl. Acad. Sci. U. S. A. 103 (2006) 8469–8474.
[24] A. Aoi, Y. Watanabe, S. Mori, M. Takahashi, G. Vassaux, T. Kodama, Herpes simplex virus thymidine kinase-mediated suicide gene therapy using nano/microbubbles and ultrasound, Ultrasound Med. Biol. 34 (2008) 425–434.
[25] Z.P. Shen, A.A. Brayman, L. Chen, C.H. Miao, Ultrasound with microbubbles enhances gene expression of plasmid DNA in the liver via intraportal delivery, Gene Ther. (2008).
[26] S. Sonoda, K. Tachibana, E. Uchino, A. Okubo, M. Yamamoto, K. Sakoda, T. Hisatomi, K.H. Sonoda, Y. Negishi, Y. Izumi, S. Takao, T. Sakamoto, Gene transfer to corneal epithelium and keratocytes mediated by ultrasound with microbubbles, Investig. Ophthalmol. Vis. Sci. 47 (2006) 558–564.
[27] K. Iwanaga, K. Tominaga, K. Yamamoto, M. Habu, H. Maeda, S. Akifusa, T. Tsujisawa, T. Okinaga, J. Fukuda, T. Nishihara, Local delivery system of cytotoxic agents to tumors by focused sonoporation, Cancer Gene Ther. 14 (2007) 354–363.
[28] R. Bekeredjian, S. Chen, P.A. Grayburn, R.V. Shohet, Augmentation of cardiac protein delivery using ultrasound targeted microbubble destruction, Ultrasound Med. Biol. 31 (2005) 687–691.
[29] R. Bekeredjian, H.F. Kuecherer, R.D. Kroll, H.A. Katus, S.E. Hardt, Ultrasound-targeted microbubble destruction augments protein delivery into testes, Urology 69 (2007) 386–389.
[30] T. Yamashita, S. Sonoda, R. Suzuki, N. Arimura, K. Tachibana, K. Maruyama, T. Sakamoto, A novel bubble liposome and ultrasound-mediated gene transfer to ocular surface: RC-1 cells in vitro and conjunctiva in vivo, Exp. Eye Res. 85 (2007) 741–748.

Author's personal copy

[31] R. Suzuki, T. Takizawa, Y. Negishi, K. Hagisawa, K. Tanaka, K. Sawamura, N. Utoguchi, T. Nishioka, K. Maruyama, Gene delivery by combination of novel liposomal bubbles with perfluoropropane and ultrasound, J. Control. Release 117 (2007) 130–136.
[32] R. Suzuki, T. Takizawa, Y. Negishi, N. Utoguchi, K. Maruyama, Effective gene delivery with novel liposomal bubbles and ultrasonic destruction technology, Int. J. Pharm. 354 (2008) 49–55.
[33] R. Suzuki, T. Takizawa, Y. Negishi, N. Utoguchi, K. Sawamura, K. Tanaka, E. Namai, Y. Oda, Y. Matsumura, K. Maruyama, Tumor specific ultrasound enhanced gene transfer in vivo with novel liposomal bubbles, J. Control. Release 125 (2008) 137–144.
[34] R. Suzuki, T. Takizawa, Y. Negishi, N. Utoguchi, K. Maruyama, Effective gene delivery with liposomal bubbles and ultrasound as novel non-viral system, J. Drug Target. 15 (2007) 531–537.
[35] J.D. Pfeifer, M.J. Wick, R.L. Roberts, K. Findlay, S.J. Normark, C.V. Harding, Phagocytic processing of bacterial antigens for class I MHC presentation to T cells, Nature 361 (1993) 359–362.
[36] K. Inaba, M. Inaba, M. Deguchi, K. Hagi, R. Yasumizu, S. Ikehara, S. Muramatsu, R.M. Steinman, Granulocytes, macrophages, and dendritic cells arise from a common major histocompatibility complex class II-negative progenitor in mouse bone marrow, Proc. Natl. Acad. Sci. U. S. A. 90 (1993) 3038–3042.
[37] D.P. Guo, X.Y. Li, P. Sun, Y.B. Tang, X.Y. Chen, Q. Chen, L.M. Fan, B. Zang, L.Z. Shao, X.R. Li, Ultrasound-targeted microbubble destruction improves the low density lipoprotein receptor gene expression in HepG2 cells, Biochem. Biophys. Res. Commun. 343 (2006) 470–474.
[38] T. Mosmann, Rapid colorimetric assay for cellular growth and survival: application to proliferation and cytotoxicity assays, J. Immunol. Methods 65 (1983) 55–63.
[39] S.E. Slezak, P.K. Horan, Cell-mediated cytotoxicity. A highly sensitive and informative flow cytometric assay, J. Immunol. Methods 117 (1989) 205–214.
[40] G. Reinhard, A. Marten, S.M. Kiske, F. Feil, T. Bieber, I.G. Schmidt-Wolf, Generation of dendritic cell-based vaccines for cancer therapy, Br. J. Cancer 86 (2002) 1529–1533.
[41] M. Kinoshita, K. Hynynen, Intracellular delivery of Bak BH3 peptide by microbubble-enhanced ultrasound, Pharm. Res. 22 (2005) 716–720.
[42] I.V. Larina, B.M. Evers, R.O. Esenaliev, Optimal drug and gene delivery in cancer cells by ultrasound-induced cavitation, Anticancer Res. 25 (2005) 149–156.
[43] M. Duvshani-Eshet, D. Adam, M. Machluf, The effects of albumin-coated microbubbles in DNA delivery mediated by therapeutic ultrasound, J. Control. Release 112 (2006) 156–166.
[44] C.M. Newman, T. Bettinger, Gene therapy progress and prospects: ultrasound for gene transfer, Gene Ther. 14 (2007) 465–475.
[45] R.K. Schlicher, H. Radhakrishna, T.P. Tolentino, R.P. Apkarian, V. Zarnitsyn, M.R. Prausnitz, Mechanism of intracellular delivery by acoustic cavitation, Ultrasound Med. Biol. 32 (2006) 915–924.
[46] P.M. Kloetzel, Antigen processing by the proteasome, Nat. Rev. Mol. Cell. Biol. 2 (2001) 179–187.

Author's personal copy

Available online at www.sciencedirect.com
ScienceDirect
Journal of Controlled Release 125 (2008) 137–144
journal of controlled release
www.elsevier.com/locate/jconrel
GENE DELIVERY

Tumor specific ultrasound enhanced gene transfer *in vivo* with novel liposomal bubbles

Ryo Suzuki [a], Tomoko Takizawa [a], Yoichi Negishi [b], Naoki Utoguchi [a], Kaori Sawamura [a], Kumiko Tanaka [a], Eisuke Namai [a], Yusuke Oda [a], Yasuhiro Matsumura [c], Kazuo Maruyama [a,*]

[a] *Department of Biopharmaceutics, School of Pharmaceutical Sciences, Teikyo University, 1091-1 Suwarashi, Sagamiko, Sagamihara, Kanagawa 229-0195, Japan*
[b] *Department of Drug and Gene Delivery System, School of Pharmacy, Tokyo University of Pharmacy and Life Science, Hachioji, Tokyo, Japan*
[c] *Investigative Treatment Division, Research Center for Innovative Oncology, National Cancer Center Hospital East, Kashiwa, Chiba, Japan*

Received 30 November 2006; accepted 19 August 2007
Available online 29 August 2007

Abstract

Bubble liposomes (liposomes which entrap an ultrasound imaging gas) may constitute a unique system for delivering various molecules efficiently into mammalian cells *in vitro*. In this study, Bubble liposomes were compared with cationic lipid (CL)–DNA complexes as potential gene delivery carriers into tumor *in vivo*. The delivery of genes by Bubble liposomes depended on the intensity of the applied ultrasound. Transfection efficiency plateaued at 0.7 W/cm^2 ultrasound intensity. Bubble liposomes efficiently transferred genes into cultured cells even when the cells were exposed to ultrasound for only 1 s. In addition, Bubble liposomes could introduce the luciferase gene more effectively than CL-DNA complexes into mouse ascites tumor cells and solid tumor tissue. We conclude that the combination of Bubble liposomes and ultrasound is a minimally-invasive and tumor specific gene transfer method *in vivo*.
© 2007 Elsevier B.V. All rights reserved.

Keywords: Liposomes; Bubble liposomes; Gene delivery; Ultrasound; Cancer

1. Introduction

In cancer gene therapy, it is important to develop the easy, safe, efficient, minimally-invasive and tissue-specific technologies of gene transfer into tumor tissue. Sonoporation is a method of gene delivery with ultrasound. Ultrasound increases the permeability of the plasma membrane and reduces the thickness of the unstirred layer of the cell surface, aiding DNA entry into cells [1,2]. Preliminary studies into the utility of ultrasound for gene delivery used frequencies in the range of 20–50 kHz [1,3]. However, these frequencies are also known to induce tissue damage and cavitation if not properly controlled [4–6]. To overcome this problem, several studies have used frequencies of 1–3 MHz, intensities of 0.5–2 W/cm^2, and pulse-modulation [7–9]. In a separate approach, a combination of therapeutic ultrasound and microbubble echo contrast agents was shown to enhance gene transfection efficiency [10–15] by effectively and directly transferring DNA into the cytosol. Microbubbles based on protein microspheres, and sugar microbubbles, are commercially available; however, although they encapsulate ultrasound contrast agents, they are too large (2–10 μm diameter) for intravascular application [16]. It has been reported that the *i.v.* injection of Optison without ultrasound exposure results in lethal embolisms in vital organs in mice [17]. Although a similar effect has not been observed in humans, it is possible that Optison can not pass through capillary vessels. Ideally, microbubbles should be smaller than red blood cells.

Liposomes can be used as drug, antigen and gene delivery carriers [18–26]. Based on liposome technology, we developed novel liposomal bubbles (Bubble liposomes) containing the ultrasound imaging gas, perfluoropropane. When coupled with ultrasound exposure, Bubble liposomes can be used as novel

* Corresponding author. Tel.: +81 42 685 3722; fax: +81 42 685 3432.
E-mail address: maruyama@pharm.teikyo-u.ac.jp (K. Maruyama).

0168-3659/$ - see front matter © 2007 Elsevier B.V. All rights reserved.
doi:10.1016/j.jconrel.2007.08.025

Author's personal copy

gene delivery agents [27]. In addition, we found out that the gene delivery was only observed at the site of ultrasound exposure. Therefore, using Bubble liposomes and ultrasound, we could establish minimally-invasive and tumor tissue-specific gene delivery. In the present study, the characteristics of Bubble liposomes as gene delivery vectors were studied, and gene transfection efficiencies into tumor *in vivo* were compared with lipofection using cationic liposomes, a common non-viral gene transfer method.

2. Materials and methods

2.1. Cells

African green monkey kidney fibroblast COS-7 cells were cultured in Dulbecco's modified Eagle's medium (DMEM; Sigma Chemical Co., St. Louis, MO) supplemented with 10% heat inactivated fetal Bovine serum (FBS, GIBCO, Invitrogen Co., Carlsbad, CA). Mouse Sarcoma-180 (S-180) cells were cultured in Eagle's medium (MEM; Sigma) supplemented with 10% heat inactivated FBS. All culture media contained 100 U/mL penicillin (Wako Pure Chemical Industries, Ltd., Osaka, Japan) and 100 μg/mL streptomycin (Wako).

2.2. Preparation of liposomes and Bubble liposomes

Liposomes composed of 1,2-distearoyl-sn-glycero-phosphatidylcholine (DSPC) (NOF Corporation, Tokyo, Japan) and 1,2-distearoyl-sn-glycero-3-phosphatidyl-ethanolamine-methoxy-polyethyleneglycol (DSPE-PEG (2 k)–OMe; NOF) (94:6 (m/m)) were prepared by reverse phase evaporation. In brief, all reagents (total lipid: 100 μmol) were dissolved in 8 mL of 1:1 (v/v) chloroform/diisopropyl ether, then 4 mL of PBS was added. The mixture was sonicated and evaporated at 65 °C. The solvent was completely removed, and the size of the liposomes was adjusted to less than 200 nm using an extruding apparatus (Northern Lipids Inc., Vancouver, BC) and sizing filters (pore sizes: 100 nm and 200 nm; Nuclepore Track-Etch Membrane, Whatman plc, UK). After sizing, the liposomes were sterilized by passing them through a 0.45 μm pore size filter (MILLEX HV filter unit, Durapore PVDF membrane, Millipore Corporation, MA). The liposome size was measured with dynamic light scattering (ELS-800, Otsuka Electronics Co., Ltd., Osaka, Japan). The average diameter of these liposomes were about 150–200 nm. Lipid concentration was measured with the Phospholipid C test wako (Wako Pure Chemical Industries). Bubble liposomes were prepared from the liposomes and perfluoropropane gas (Takachiho Chemical Ind. Co. Ltd., Tokyo, Japan). In brief, 5 mL sterilized vials containing 2 mL of the liposome suspension (lipid concentration: 1 mg/mL) were filled with perfluoropropane, capped and then supercharged with 7.5 mL of perfluoropropane. The vial was placed in a bath-type sonicator (42 kHz, 100 W; BRANSONIC 2510J-DTH, Branson Ultrasonics Co., Danbury, CT) under the condition of positive pressure with perfuluoropropane in the vial under the condition of positive pressure with perfuluoropropane in the vial for 5 min to form the Bubble liposomes.

2.3. Microscopic observation of Optison and Bubble liposomes and size distribution

Optison (NEPA GENE, CO., LTD., Chiba, Japan) or Bubble liposomes were placed on glass slides, covered with a cover slip and observed with a microscope (Leica MICROSYSTEMS, Wetzlar, Germany) using a darklite illuminator (NEPA GENE). The size distribution of Optison and Bubble liposomes was measured by dynamic light scattering (ELS-800).

2.4. Transmission electron microscopy of Bubble liposomes

Bubble liposomes were suspended into sodium alginate solution (0.2% (w/v) in PBS). This suspension was dropped into calcium chloride solution (100 mM) to hold Bubble liposomes within calcium alginate gel. Then, the beads of calcium alginate gel containing Bubble liposomes were prefixed with 2% glutaraldehyde solution in 0.1 M Cacodylate buffer, post-fixed with 2% OsO_4, dehydrated with an ethanol series, and then embedded in Epan812 (polymerized at 60 °C). Ultrathin sections were made with an ultramicrotome at a thickness of 60–80 nm. Ultrathin sections were mounted on 200 mesh copper grids. They were stained with 2% uranyl acetate for 5 min and Pb for 5 min. The samples were observed with JEOL JEM12000EX at 100 kV. The treatment after prefixation was carried out in Hanaichi Ultrastructure Research Institute Co.,Ltd (Aichi, Japan).

2.5. Transfection of plasmid DNA into cells using Bubble liposomes

Luciferase cording plasmid DNA (pCMV-Luc), COS-7 cells (1×10^5 cells) and Bubble liposomes (60 μg) were suspended in culture medium (500 μL) with 10% FBS in 2 mL polypropylene tubes. The suspension was ultrasonicated using a Sonopore 4000 (6 mm diameter probe; NEPA GENE) sonicator under various conditions. The cells were washed twice with PBS, resuspended in fresh culture medium and cultured in 48-well plates for 2 days.

2.6. Transfection of plasmid DNA into cells by lipofection

Plasmid DNA (pCMV-Luc, 0.25 μg) and Lipofectin (1.25 μg) (Invitrogen) were mixed and complexed according to the manufacturer's instructions. The complex was added to COS-7 cell suspensions (1×10^5 cells/500 μL/ tube) containing various concentrations of serum for 10 s. The cells were washed twice with PBS, resuspended in fresh culture medium and cultured in 48-well plates for 2 days.

2.7. In vivo gene delivery into mouse ascites tumor cells

S-180 cells (1×10^6 cells) were *i.p.* injected into ddY mice (4 weeks old, male) (Sankyo Labo Service Corporation, Tokyo, Japan) on day 0. When S-180 cells grew as the ascites tumor in mice after 8 days of the injection [28], the mice were anaesthetized with NEMBUTAL (50 mg/kg) (Dainippon

Author's personal copy

Sumitomo Pharma, Osaka, Japan), then injected with 510 μL of pCMV-Luc (10 μg) and Bubble liposomes (500 μg) in PBS. Ultrasound (frequency: 1 MHz, duty: 50%; intensity: 1.0 W/cm^2, time: 1 min) was transdermally applied to the abdominal area using a Sonopore 3000 ultrasonicator with a probe of diameter 20mm (NEPA GENE). In other experiments, pCMV-Luc (10μg) and Lipofectin (50μg) or Lipofectamine 2000 (50μg) were mixed and complexed according to the manufacturer's instructions. The complex was suspended in PBS (510μL) and injected into the peritoneal cavities of mice. After 2days, S-180 cells were recovered from the abdomens of the mice. Then, the recovered cells were lysed in the lysis buffer (0.1M Tris–HCl (pH 7.8), 0.1% Triton X-100, 2mM EDTA) and luciferase activity was determined.

2.8. In vivo gene delivery into mouse footpad solid tumor

S-180 cells (1×10^6 cells) were inoculated into the left footpad of ddY mice (5 weeks old, male). At day 4, when the thickness of the footpad was over 3.5 mm (normal thickness was about 2 mm), the left femoral artery was exposed. One hundred μL of pCMV-Luc (10 μg) with or without Bubble liposomes (100 μg) were injected into femoral artery using 30-gauge needle. In the same time, ultrasound (frequency: 0.7 MHz, duty: 50%; intensity: 1.2 W/cm^2, time: 2 min) was transdermally applied to the tumor tissue using a Sonopore 4000 ultrasonicator with a probe of diameter 8 mm (NEPAGENE). The needle hole was then closed with an adhesive agent (Aron Alpha; Sankyo, Tokyo, Japan) and skin was put in a suture. In other samples, pCMV-Luc (10 μg) and Lipofectamine 2000 (25 μg) (Invitrogen Corporation, Carlsbad, CA) were mixed and complexed according to manual of Lipofectamine 2000. The complex were suspended in PBS (100 μL) and injected into femoral artery of mice. After 2 days of injection, the mice were sacrificed and the tumor tissues were collected. Then, the tumor tissues were homogenated in the lysis buffer and luciferase activity was determined.

2.9. Luciferase assay

Luciferase activity was measured using a luciferase assay system (Promega, Madison, WI) and a luminometer (TD-20/20, Turner Designs, Sunnyvale, CA). Activity is reported in relative light units (RLU) per mg protein.

2.10. In vivo Luciferase imaging

The mice were anaesthetized and *i.p.* injected with D-luciferin (150 mg/kg) (Xenogen, Corporation, CA). After 10 min, luciferase expression was observed with *in vivo* luciferase imaging system (IVIS) (Xenogen Corporation).

2.11. Hemolysis assay

Mouse red blood cells (2.5×10^8 cells/500 μL) were exposed with ultrasound (frequency: 0.7 MHz, Duty: 50%, Intensity: 0.5–1.5 W/cm^2, Time: 10 s.) in absent or present of Bubble liposomes. The red blood cell suspension was centrifuged for 10 min at 3000 rpm. Then, absorbance ($A_{540\ nm}$) of the supernatant was measured. The rate of hemolysis was calculated as follows: % of hemolysis=($A_{540\ nm}$ of experimental group $-A_{540\ nm}$ of non-treated group)/($A_{540\ nm}$ of hypotonic solution treated group $-A_{540\ nm}$ of non-treated group)$\times$100.

2.12. In vivo studies

All experimental protocols for animal studies were in accordance with the Principle of Laboratory Animal Care in Teikyo University.

2.13. Statistical analysis

Differences in luciferase activity between experimental groups were compared with non-repeated measures ANOVA and Dunnett's test.

3. Results and discussion

The use of non-viral vectors is attractive as a safe, clinically acceptable gene therapy technique. In addition, non-viral vectors should be easy to prepare and use. However, most non-viral vectors deliver plasmid DNA into cells via endocytosis, followed by plasmid DNA degradation in the endosomes. Consequently, non-viral vectors often result in low gene delivery efficiency. It has been reported that new types of non-viral vectors can induce the escape of genes from endosomes [29–31] and directly deliver genes into the cytosol via a fusion mechanism [28,32]. In addition, microbubbles and ultrasound have been investigated with a view to improving the transfection efficiency of non-viral vectors. Gene delivery using a combination of microbubbles such as Optison and ultrasound has been widely reported. In order for extracellular plasmid DNA to be directly and effectively delivered into the cytosol, transient pores in the cell membrane must be formed by cavitation. However, conventional microbubbles are very large, with most greater than 2 μm in diameter [16]. Actually, our observations of Optison using a microscope and a darklite illuminator showed some bubbles more than 10 μm in diameter (Fig. 1(a)). In the measurement of the size distribution, there were some large microbubbles (Fig. 1d)). Tsunoda et al. pointed out that these large bubbles might cause lethal embolism in some vital organs [17]. In contrast, most Bubble liposomes were much smaller than Optison, with average diameters less than 2 μm (Fig. 1(b, e)). The injection of 1 mg of Bubble liposomes into the tail veins of mice was not lethal (data not shown), suggesting that Bubble liposomes may not cause lethal embolism. To confirm the structure of Bubble liposomes, we observed Bubble liposome with transmission electron microscopy (Fig. 1(c)). Interestingly, there were nanobubbles into lipid bilayer. From this result, it was thought that Bubble liposomes were different from conventional microbubbles which was the echo gas wrapped with lipid mono-layer. Kodama T. et al. and Klibanov A.L. et al. reported about microbubbles using distearoylphospatidylcholine and PEG-

Author's personal copy

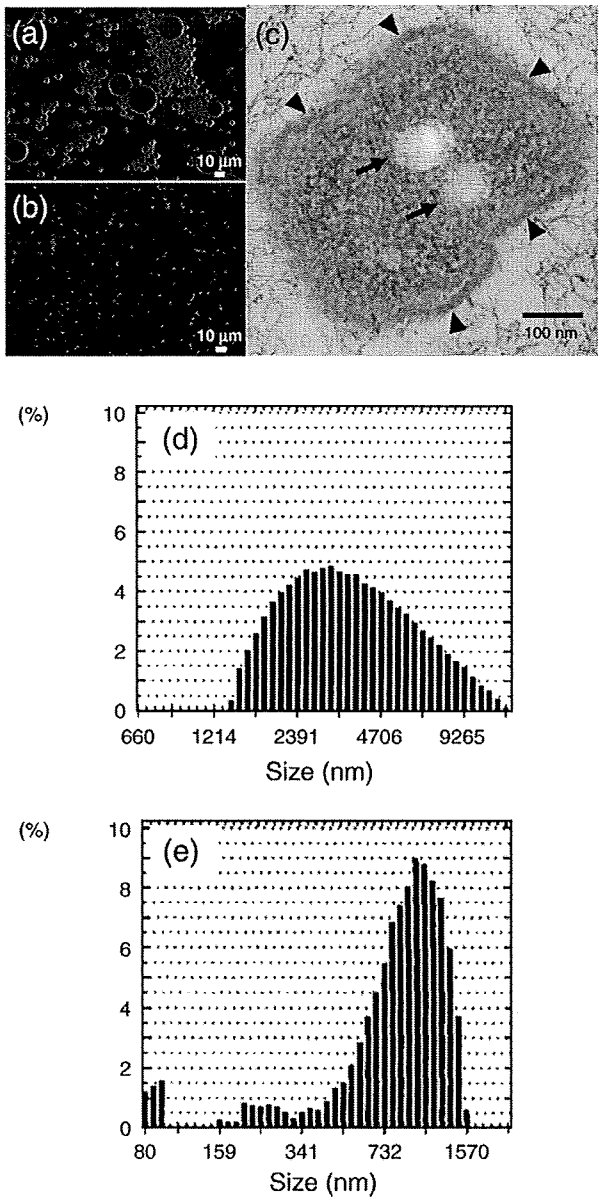

Fig. 1. Microscopy of Optison and Bubble liposomes. Optison (a) and Bubble liposomes (b) were observed with a microscope using a darklite illuminator. Original magnification ×400. Bubble liposomes (c) were observed with a transmission electric microscope at 100 kV. Original magnification ×50,000. Arrow head shows lipid bi-layer and arrow shows perfluoropropane nanobubble. The size distribution of Optison (d) and Bubble liposomes (e).

stearate [33,34]. These microbubbles were made by being stabilized hydrophobic echo gas with amphipathic molecules such as lipid and surfactant. In our method, it was thought that liposomes were reconstituted by sonication under the condition of supercharge with perfluoropropane in the 5 mL vial container. At the same time, perfluoropropane would be entrapped within lipids like micelles, which were made by DSPC and DSPE-PEG (2 k)-OMe from liposome composition, to form nanobubbles. The lipid nanobubbles were encapsulated within the reconstituted liposomes (Fig. 1(c)), which sizes were changed into around 1 μm (Fig. 1(b,e)) from 150–200 nm of original. In addition, we evaluated about the stability of Bubble liposomes by transfection efficiency with sonoporation (Fig. 2). The efficiency gradually decreased according to storage time. We also observed the aspect and ultrasound imaging of Bubble liposomes. The suspension of Bubble liposomes gradually became clear in aspects, resulted in decreasing the echo signal according to storage time (data not shown). These results suggested that perfluoropropane was gradually degassed from Bubble liposomes. Therefore, we used fresh Bubble liposomes in all experiments.

Previously, we reported that Bubble liposomes could induce cavitation and deliver plasmid DNA into various types of cells [27]. In order to examine what conditions are necessary for Bubble liposomes to efficiently deliver genes, transfection efficiency was assessed using Bubble liposomes combined with various levels of ultrasound exposure (Fig. 3(a)). COS-7 cells were exposed to various intensities of ultrasound in the presence of Bubble liposomes for 10 s. Gene transfection efficiency increased with increasing ultrasound intensity and reached a plateau at 0.7 W/cm^2. No cytotoxicity was evident even at 2.5 W/cm^2 (data not shown). The length of ultrasound exposure required to achieve gene expression was examined by measuring gene expression after 0, 1, 5 and 10 s of exposure (Fig. 3(b)). Surprisingly, gene expression was observed after 1 s of ultrasound exposure in the presence of Bubble liposomes. Transfection efficiency depended on ultrasound exposure time and reached a plateau after 5 s exposure. Efficiency was found to depend on both ultrasound intensity and exposure time (Fig. 3), indicating that Bubble liposomes can rapidly induce gene delivery while requiring only weak ultrasound, and without inducing cytotoxicity. Five seconds or 0.7 W/cm^2 of ultrasound exposure resulted in maximal gene expression, presumably due to bubble cavitation.

The transfection efficiency of some cationic non-viral vectors is significantly decreased in the presence of serum

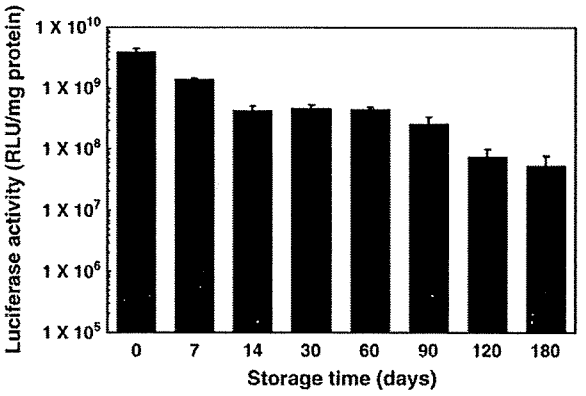

Fig. 2. Stability of Bubble liposomes. After preparation of Bubble liposomes, the vial containing Bubble liposomes was put in the refrigerator for each period. After storage, the transfection efficiency was measured with each samples. COS-7 cells (1×10^5 cells/500 μL) were mixed with pCMV-Luc (5 μg) and Bubble liposomes (60 μg). The cell mixture was exposed to ultrasound (frequency: 2 MHz, duty: 50%, burst rate: 2 Hz, intensity: 2.5 W/cm^2, time: 10 s.). The cells were washed and cultured for 2 days, then luciferase activity was determined as described in Materials and methods. Each bar represents the mean±S.D. for triplicate.

Author's personal copy

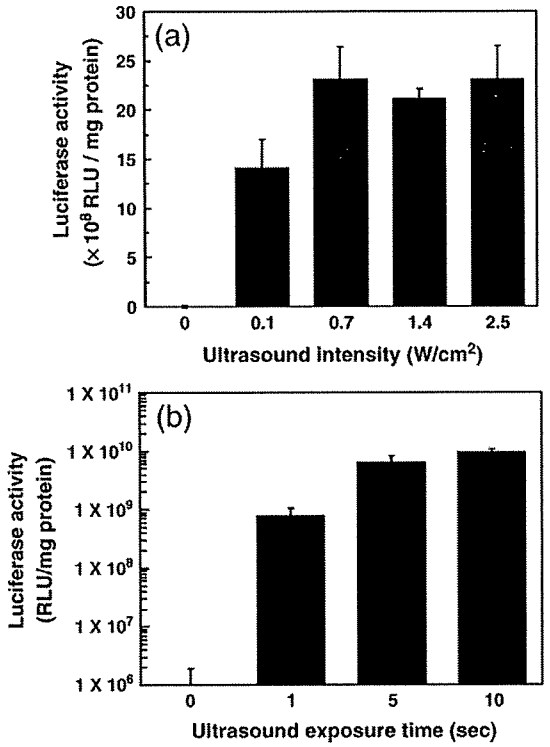

Fig. 3. Effect of ultrasound conditions on transfection efficiency with Bubble liposomes. COS-7 cells (1×10^5 cells/500 μL) were mixed with pCMV-Luc (5 μg) and Bubble liposomes (60 μg). The cell mixture was exposed to ultrasound (a): (frequency: 2 MHz, duty: 50%, burst rate: 2 Hz, intensity: 0–2.5 W/cm^2, time: 10 s.) or (b): (frequency: 2 MHz, duty: 50%, burst rate: 2 Hz, intensity: 2.5 W/cm^2, time: 0–10 s.). The cells were washed and cultured for 2 days, then luciferase activity was determined as described in Materials and methods. Each bar represents the mean±S.D. for triplicate.

due to an interaction between serum proteins and the cationic vectors [28]. Whereas, transfection efficiency with the combination of Bubble liposomes and ultrasound did not decrease even in the presence of 50% serum in *in vitro* study [27]. In the next examination, we examined whether Bubble liposomes could deliver plasmid DNA into S-180 ascites tumor cells in living animals after local injection (Fig. 4). In this examination, we compared the transfection efficiency with Bubble liposomes or cationic liposomes such as Lipofectin and Lipofectamine 2000. Luciferase expression was low in the mice treated with lipofectin-plasmid DNA complexes prepared by the traditional lipofection method, presumably because the complexes were associated with various proteins in the peritoneal cavity. On the other hand, luciferase expression increased in the mice treated with Lipofectamine 2000-plasmid DNA complexes compare with Lipofectin, because it was known that LF2000 was better than Lipofectin for gene delivery in the presence of serum. In addition, luciferase expression in mice treated with plasmid DNA, Bubble liposomes and ultrasound exposure was higher than that in the mice treated with Lipofectamine 2000-plasmid DNA complexes. This result supported the previous our report. In short, it was thought that Bubble liposomes and ultrasound was not affected by proteins existing in the peritoneal cavity and this method immediately and directly delivered plasmid DNA into cells with the mechanism which was not endocytosis pathway in lipofection method. We also confirmed that ultrasound combined with Bubble liposomes was effective at delivering genes to other tissues in the peritoneal cavity such as stomach, kidney, liver, spleen, intestine, diaphragm, pancreas, peritoneum and mesentery. Luciferase activity in these tissues was much lower than that observed in the S-180 cells (less than 130 RLU/mg protein).

Mizuguchi et al. reported about the effective cancer gene therapy by cytokine provision in the local area via gene delivery into arteries leading to tumor or arteries in tumor tissue [35]. Previously, we succeeded the gene delivery into artery of ultrasound exposure site with Bubble liposomes [27]. Therefore, we thought that our technology could be applied to establish the tumor tissue specific gene delivery. In this time, we attempted to deliver plasmid DNA to solid tumor via the injection into the artery that lead to tumor (Fig. 5). In Fig. 4, Lipofectin did not work well as gene delivery tool. In this study, we only used Lipofectamine 2000 as a control. In the mice treated with plasmid DNA and ultrasound, luciferase expression was same low level in the mice of plasmid DNA injection. And, luciferase expression was also low level in the mice treated with Lipofectamine 2000 and plasmid DNA complex, although the complex could be induced into S-180 ascites tumor cells. Generally, enough time is necessary for the complex to bind to cell surface and deliver plasmid DNA into cells. In this case, there was no time for the complex to retain in tumor tissue after injection because of blood stream and it would be resulted in

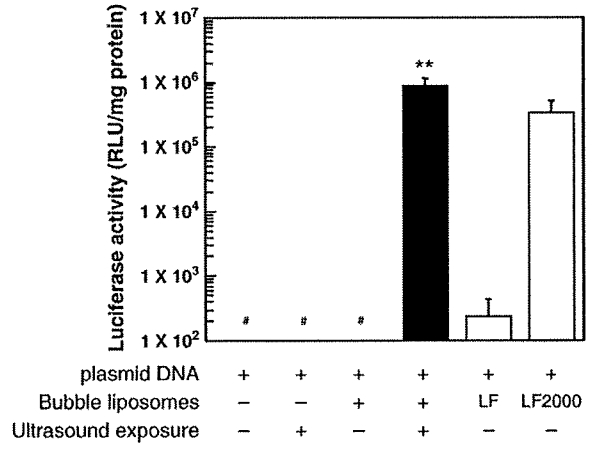

Fig. 4. *In vivo* gene delivery into mouse ascites tumor cells with Bubble liposomes. S-180 cells (1×10^6 cells) were i.p. injected into ddY mice. After 8 days, the mice were anaesthetized, then injected with 510 μL of pCMV-Luc (10 μg) and Bubble liposomes (500 μg) in PBS. Ultrasound (frequency: 1 MHz, duty: 50%; intensity: 1.0 W/cm^2, time: 1 min) was transdermally applied to the abdominal area. In another experiment, pCMV-Luc (10 μg) — Lipofectin (50 μg) or Lipofectamine 2000 (50 μg) complex was suspended in PBS (510 μL) and injected into the peritoneal cavity of mice. After 2 days, S-180 cells were recovered from the abdomens of the mice. Luciferase activity was determined as described in Materials and methods. Each bar represents the mean±S.D. for three to six mice/group. $^{**}P<0.01$ compared to the group treated with plasmid DNA, Bubble liposomes, ultrasound exposure or lipofection with Lipofectin or Lipofectamine 2000. LF, Lipofectin. LF2000, Lipofectamine 2000. #$<10^2$ RLU/mg protein.

Author's personal copy

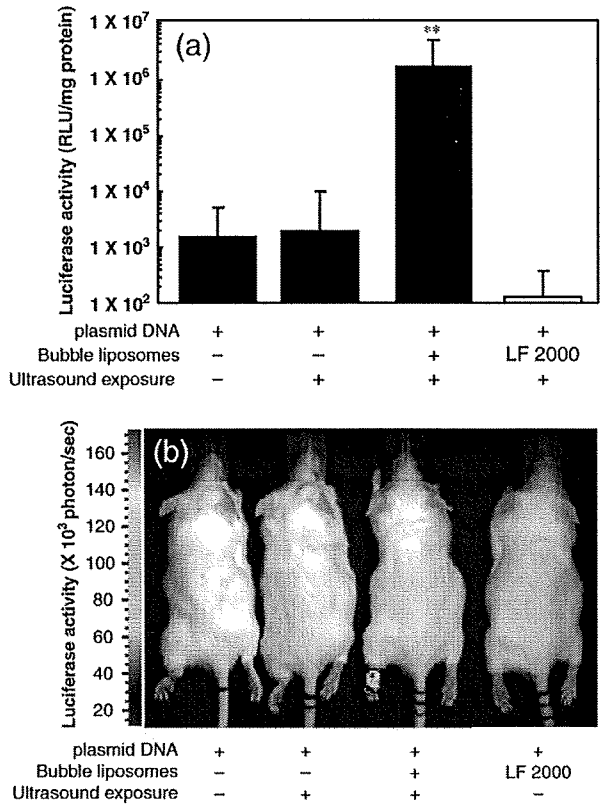

Fig. 5. *In vivo* gene delivery into mouse solid tumor with Bubble liposomes. S-180 cells (1×10^6 cells) were inoculated into left footpad of ddY mice. After 4 days, the mice were anaesthetized, then injected with 100 mL of pCMV-Luc (10 μg) in absent or present of Bubble liposomes (100 μg) in PBS. Ultrasound (frequency: 0.7 MHz, duty: 50%; intensity: 1.2 W/cm^2, time: 1 min) was transdermally exposed to tumor tissue. In another experiment, pCMV-Luc (10 μg) — Lipofectamine 2000 (25 μg) complex was suspended in PBS (100 μL) and injected into the left femoral artery. After 2 days, tumor tissue was recovered the mice. Luciferase activity was determined as described in Materials and methods. (a) Luciferase activity in solid tumor. Each bar represents the mean±S.D. for five mice/group. $^{**}P<0.01$ compared to the group treated with plasmid DNA, ultrasound exposure or Lipofectamine 2000. (b) *In vivo* luciferase imaging in the solid tumor bearing mice. The photon counts are indicated by the pseudo-color scales. LF 2000, Lipofectamine 2000.

low efficiency of transfection. On the other hand, luciferase expression in the combination of Bubble liposomes and ultrasound was much higher than that in other group (Fig. 5(a)). Koch et al. reported that the combination of ultrasound and microbubble (Levovist) enhanced lipoplex-mediated cell transfection efficiency *in vitro* and also severely damaged most cells. [36]. Therefore, we attempted to confirm the enhancement of transcfection efficiency with Lipofectamine 2000 by Bubble liposomes and ultrasound in the condition without cell damage. The transfection efficiency with lipoplex was not enhanced with Bubble liposomes and ultrasound *in vitro* and *in vivo* (data not shown). The size of Lipofectamine 2000-plasmid DNA complexes was larger than that of naked plasmid DNA by forming the spaghetti–meatball like structure. We guessed that it was difficult for the complexes to enter into cytosol via transient pore on the membrane with cavitation of Bubble liposomes in the condition without cell damage. In the Koch's report, ultrasound was exposed to *in vitro* cells for 60 s with Levovist (20 and 200 mg/mL). In this study, Bubble liposomes (1 mg/mL) were injected into the femoral artery. The concentration of Bubble liposomes would be much lower than that of Levovist because of the dilution of Bubble liposomes in the blood. In addition, the time of ultrasound exposure to Bubble liposomes was very short because of blood flow. Therefore, I thought that the transfection efficiency in the combination of cavitation with Bubble liposomes and lipoplexes was not enhanced. To evaluate gene expression site, we observed luciferase expression with luciferase *in vivo* imaging system (Fig. 5(b)). In the mice treated with Bubble liposomes and ultrasound, luciferase expression was observed in the tumor tissue because of inducing cavitation at ultrasound exposure site. Then, there were a possibility of hemolysis by the cavitation of Bubble liposomes in artery. We examined about hemolytic effect in the treatment of Bubble liposomes and ultrasound (Fig. 6). When the ultrasound was exposed to red blood cell with or without Bubble liposomes *in vitro*, serious hemolysis was not induced. These results suggested that this gene delivery system was important method to achieve tumor specific gene delivery without serious damage.

Plasmid DNA was effectively delivered into S-180 ascites tumor cells and solid tumor tissues with Bubble liposomes and ultrasound, although plasmid DNA did not form a complex with Bubble liposomes because Bubble liposomes were made of neutral charge lipids and modified polyethylene glycol on the surface, and existed free *in vivo*. These results could be explained from Fig. 3. In short, it is thought that Bubble liposomes can immediately and effectively deliver plasmid DNA into cells *in vivo* before the plasmid DNA is degraded by DNase. A mixture of plasmid DNA and Bubble liposomes was injected into mice, and the plasmid DNA was delivered to a specific area of the abdomen or solid tumor tissue by local exposure to ultrasound, suggesting that gene targeting can be induced at a site by exposure to ultrasound. In future studies, we intend to establish minimally-invasive and tissue-specific gene delivery with Bubble liposomes after systemic injection.

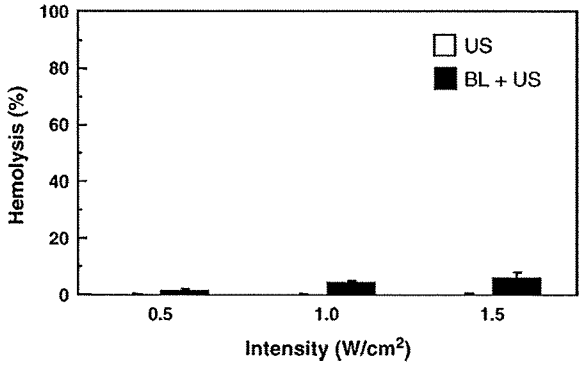

Fig. 6. Hemolysis of red blood cells by Bubble liposomes and ultrasound. Mouse red blood cells (2.5×10^8 cells/ 500 mL) were exposed with ultrasound (frequency: 0.7 MHz, Duty: 50%, Intensity: 0.5–1.5 W/cm^2, Time: 10 s.) in absent or present of Bubble liposomes. Hemolysis was assessed as described in Materials and methods. Each bar represents the mean±S.D. for triplicate.

Author's personal copy

The present study showed that Bubble liposomes can be a more effective gene delivery tools into tumor *in vivo* than conventional lipofection. Moreover, Bubble liposomes are an attractive gene delivery approach in cancer gene therapy as the method is minimally-invasive and tumor specific gene transfer, requiring only exposure to ultrasound applied to the surface of the body.

Acknowledgements

We are grateful to Dr. Katsuro Tachibana (Department of Anatomy, School of Medicine, Fukuoka University) for technical advice regarding the induction of cavitation with ultrasound, to Mr. Katsutoshi Kurosawa, Mr. Takamichi Todoroki, Ms. Hitomi Tamagawa (Department of Biopharmaceutics, School of Pharmaceutical Sciences, Teikyo University) for excellent technical assistance, to Dr. Akinori Suginaka (NOF CORPORATION) for technical advice regarding lipids and for providing the lipids, and to Mr. Yasuhiko Hayakawa, Mr. Takahiro Yamauchi and Mr. Kosho Suzuki (NEPA GENE CO., LTD.) for technical advice regarding ultrasound exposure.

This study was supported by an Industrial Technology Research Grant (04A05010) in 2004 from the New Energy and Industrial Technology Development Organization (NEDO) of Japan, a Grant-in-Aid for Young Scientists (160700392, 19700423), Exploratory Research (16650126) from the Japan Society for the Promotion of Science and a Research on Advanced Medical Technology (17070301) in Health and Labour Sciences Research Grants from Ministry of Health, Labour and Welfare.

References

[1] M. Fechheimer, J.F. Boylan, S. Parker, J.E. Sisken, G.L. Patel, S.G. Zimmer, Transfection of mammalian cells with plasmid DNA by scrape loading and sonication loading, Proc. Natl. Acad. Sci. U. S. A. 84 (1987) 8463–8467.

[2] M.W. Miller, D.L. Miller, A.A. Brayman, A review of in vitro bioeffects of inertial ultrasonic cavitation from a mechanistic perspective, Ultrasound Med. Biol. 22 (1996) 1131–1154.

[3] M. Joersbo, J. Brunstedt, Protein synthesis stimulated in sonicated sugar beet cells and protoplasts, Ultrasound Med. Biol. 16 (1990) 719–724.

[4] H.R. Guzman, A.J. McNamara, D.X. Nguyen, M.R. Prausnitz, Bioeffects caused by changes in acoustic cavitation bubble density and cell concentration: a unified explanation based on cell-to-bubble ratio and blast radius, Ultrasound Med. Biol. 29 (2003) 1211–1222.

[5] D.L. Miller, S.V. Pislaru, J.E. Greenleaf, Sonoporation: mechanical DNA delivery by ultrasonic cavitation, Somat. Cell Mol. Genet. 27 (2002) 115–134.

[6] W. Wei, B. Zheng-zhong, W. Yong-jie, Z. Qing-wu, M. Ya-lin, Bioeffects of low-frequency ultrasonic gene delivery and safety on cell membrane permeability control, J. Ultrasound. Med. 23 (2004) 1569–1582.

[7] M. Duvshani-Eshet, M. Machluf, Therapeutic ultrasound optimization for gene delivery: a key factor achieving nuclear DNA localization, J. Control Release 108 (2005) 513–528.

[8] H.J. Kim, J.F. Greenleaf, R.R. Kinnick, J.T. Bronk, M.E. Bolander, Ultrasound-mediated transfection of mammalian cells, Hum. Gene Ther. 7 (1996) 1339–1346.

[9] D.B. Tata, F. Dunn, D.J. Tindall, Selective clinical ultrasound signals mediate differential gene transfer and expression in two human prostate cancer cell lines: LnCap and PC-3, Biochem. Biophys. Res. Commun. 234 (1997) 64–67.

[10] W.J. Greenleaf, M.E. Bolander, G. Sarkar, M.B. Goldring, J.F. Greenleaf, Artificial cavitation nuclei significantly enhance acoustically induced cell transfection, Ultrasound Med. Biol. 24 (1998) 587–595.

[11] T. Li, K. Tachibana, M. Kuroki, M. Kuroki, Gene transfer with echo-enhanced contrast agents: comparison between Albunex, Optison, and Levovist in mice-initial results, Radiology 229 (2003) 423–428.

[12] R.V. Shohet, S. Chen, Y.T. Zhou, Z. Wang, R.S. Meidell, R.H. Unger, P.A. Grayburn, Echocardiographic destruction of albumin microbubbles directs gene delivery to the myocardium, Circulation 101 (2000) 2554–2556.

[13] S. Sonoda, K. Tachibana, E. Uchino, A. Okubo, M. Yamamoto, K. Sakoda, T. Hisatomi, K.H. Sonoda, Y. Negishi, Y. Izumi, S. Takao, T. Sakamoto, Gene transfer to corneal epithelium and keratocytes mediated by ultrasound with microbubbles, Investig. Ophthalmol. Vis. Sci. 47 (2006) 558–564.

[14] Y. Taniyama, K. Tachibana, K. Hiraoka, M. Aoki, S. Yamamoto, K. Matsumoto, T. Nakamura, T. Ogihara, Y. Kaneda, R. Morishita, Development of safe and efficient novel nonviral gene transfer using ultrasound: enhancement of transfection efficiency of naked plasmid DNA in skeletal muscle, Gene Ther. 9 (2002) 372–380.

[15] Y. Taniyama, K. Tachibana, K. Hiraoka, T. Namba, K. Yamasaki, N. Hashiya, M. Aoki, T. Ogihara, K. Yasufumi, R. Morishita, Local delivery of plasmid DNA into rat carotid artery using ultrasound, Circulation 105 (2002) 1233–1239.

[16] J.R. Lindner, Microbubbles in medical imaging: current applications and future directions, Nat. Rev. Drug Discov. 3 (2004) 527–532.

[17] S. Tsunoda, O. Mazda, Y. Oda, Y. Iida, S. Akabame, T. Kishida, M. Shin-Ya, H. Asada, S. Gojo, J. Imanishi, H. Matsubara, T. Yoshikawa, Sonoporation using microbubble BR14 promotes pDNA/siRNA transduction to murine heart, Biochem. Biophys. Res. Commun. 336 (2005) 118–127.

[18] M. Harata, Y. Soda, K. Tani, J. Ooi, T. Takizawa, M. Chen, Y. Bai, K. Izawa, S. Kobayashi, A. Tomonari, F. Nagamura, S. Takahashi, K. Uchimaru, T. Iseki, T. Tsuji, T.A. Takahashi, K. Sugita, S. Nakazawa, A. Tojo, K. Maruyama, S. Asano, CD19-targeting liposomes containing imatinib efficiently kill Philadelphia chromosome-positive acute lymphoblastic leukemia cells, Blood 104 (2004) 1442–1449.

[19] O. Ishida, K. Maruyama, H. Tanahashi, M. Iwatsuru, K. Sasaki, M. Eriguchi, H. Yanagie, Liposomes bearing polyethyleneglycol-coupled transferrin with intracellular targeting property to the solid tumors in vivo, Pharm. Res. 18 (2001) 1042–1048.

[20] K. Kawamura, N. Kadowaki, R. Suzuki, S. Udagawa, S. Kasaoka, N. Utoguchi, T. Kitawaki, N. Sugimoto, N. Okada, K. Maruyama, T. Uchiyama, Dendritic cells that endocytosed antigen-containing IgG-liposomes elicit effective antitumor immunity, J. Immunother. 29 (2006) 165–174.

[21] K. Maruyama, E. Holmberg, S.J. Kennel, A. Klibanov, V.P. Torchilin, L. Huang, Characterization of in vivo immunoliposome targeting to pulmonary endothelium, J. Pharm. Sci. 79 (1990) 978–984.

[22] K. Maruyama, O. Ishida, S. Kasaoka, T. Takizawa, N. Utoguchi, A. Shinohara, M. Chiba, H. Kobayashi, M. Eriguchi, H. Yanagie, Intracellular targeting of sodium mercaptoundecahydrododecaborate (BSH) to solid tumors by transferrin-PEG liposomes, for boron neutron-capture therapy (BNCT), J. Control. Release 98 (2004) 195–207.

[23] K. Maruyama, S.J. Kennel, L. Huang, Lipid composition is important for highly efficient target binding and retention of immunoliposomes, Proc. Natl. Acad. Sci. U. S. A. 87 (1990) 5744–5748.

[24] H. Yanagie, K. Maruyama, T. Takizawa, O. Ishida, K. Ogura, T. Matsumoto, Y. Sakurai, T. Kobayashi, A. Shinohara, J. Rant, J. Skvarc, R. Ilic, G. Kuhne, M. Chiba, Y. Furuya, H. Sugiyama, T. Hisa, K. Ono, H. Kobayashi, M. Eriguchi, Application of boron-entrapped stealth liposomes to inhibition of growth of tumour cells in the in vivo boron neutron-capture therapy model, Biomed. Pharmacother. 60 (2006) 43–50.

[25] H. Yanagie, K. Ogura, K. Takagi, K. Maruyama, T. Matsumoto, Y. Sakurai, J. Skvarc, R. Illic, G. Kuhne, T. Hisa, I. Yoshizaki, K. Kono, Y. Furuya, H. Sugiyama, H. Kobayashi, K. Ono, K. Nakagawa, M. Eriguchi, Accumulation of boron compounds to tumor with polyethylene-glycol binding liposome by using neutron capture autoradiography, Appl. Radiat. Isotopes 61 (2004) 639–646.

[26] H. Hatakeyama, H. Akita, K. Kogure, M. Oishi, Y. Nagasaki, Y. Kihira, M. Ueno, H. Kobayashi, H. Kikuchi, H. Harashima, Development of a novel

Author's personal copy

systemic gene delivery system for cancer therapy with a tumor-specific cleavable PEG-lipid, Gene Ther. 14 (2007) 68–77.
[27] R. Suzuki, T. Takizawa, Y. Negishi, K. Hagisawa, K. Tanaka, K. Sawamura, N. Utoguchi, T. Nishioka, K. Maruyama, Gene delivery by combination of novel liposomal bubbles with perfluoropropane and ultrasound, J. Control. Release 117 (2007) 130–136.
[28] H. Mizuguchi, T. Nakagawa, M. Nakanishi, S. Imazu, S. Nakagawa, T. Mayumi, Efficient gene transfer into mammalian cells using fusogenic liposome, Biochem. Biophys. Res. Commun. 218 (1996) 402–407.
[29] K. Kono, Y. Torikoshi, M. Mitsutomi, T. Itoh, N. Emi, H. Yanagie, T. Takagishi, Novel gene delivery systems: complexes of fusigenic polymer-modified liposomes and lipoplexes, Gene Ther. 8 (2001) 5–12.
[30] N. Sakaguchi, C. Kojima, A. Harada, K. Koiwai, K. Shimizu, N. Emi, K. Kono, Enhancement of transfection activity of lipoplexes by complexation with transferrin-bearing fusogenic polymer-modified liposomes, Int. J. Pharm. 325 (2006) 186–190.
[31] T. Kakudo, S. Chaki, S. Futaki, I. Nakase, K. Akaji, T. Kawakami, K. Maruyama, H. Kamiya, H. Harashima, Transferrin-modified liposomes equipped with a pH-sensitive fusogenic peptide: an artificial viral-like delivery system, Biochemistry 43 (2004) 5618–5628.
[32] M. Kondoh, T. Matsuyama, R. Suzuki, H. Mizuguchi, T. Nakanishi, S. Nakagawa, Y. Tsutsumi, M. Nakanishi, M. Sato, T. Mayumi, Growth inhibition of human leukemia HL-60 cells by an antisense phosphodiester oligonucleotide encapsulated into fusogenic liposomes, Biol. Pharm. Bull. 23 (2000) 1011–1013.
[33] H. Leong-Poi, J. Christiansen, A.L. Klibanov, S. Kaul, J.R. Lindner, Noninvasive assessment of angiogenesis by ultrasound and microbubbles targeted to alpha(v)-integrins, Circulation 107 (2003) 455–460.
[34] M. Takahashi, K. Kido, A. Aoi, H. Furukawa, M. Ono, T. Kodama, Spinal gene transfer using ultrasound and microbubbles, J. Control. Release 117 (2007) 267–272.
[35] H. Mizuguchi, T. Nakagawa, S. Toyosawa, M. Nakanishi, S. Imazu, T. Nakanishi, Y. Tsutsumi, S. Nakagawa, T. Hayakawa, N. Ijuhin, T. Mayumi, Tumor necrosis factor alpha-mediated tumor regression by the in vivo transfer of genes into the artery that leads to tumors, Cancer Res. 58 (1998) 5725–5730.
[36] S. Koch, P. Pohl, U. Cobet, N.G. Rainov, Ultrasound enhancement of liposome-mediated cell transfection is caused by cavitation effects, Ultrasound Med. Biol. 26 (2000) 897–903.